Analyst

Recent Advances in Electrochemical Detection of Reactive Oxygen Species: A Review

Journal:	*Analyst*
Manuscript ID	AN-CRV-12-2024-001533.R1
Article Type:	Critical Review
Date Submitted by the Author:	17-Feb-2025
Complete List of Authors:	Ghaedamini, Hamidreza; The University of Toledo, Kim, Dong-Shik ; The University of Toledo

Recent Advances in Electrochemical Detection of Reactive Oxygen Species: A Review

Hamidreza Ghaedamini[1], Dong-Shik Kim[1,z]

[1] Department of Chemical Engineering, University of Toledo, Toledo, OH, 43606, USA

[z] Corresponding author: dong.kim@utoledo.edu +1-419-530-8084

Abstract

Reactive oxygen species (ROS) are mainly generated as a result of cellular metabolism in plants and animals, playing a crucial role in cellular signaling mechanisms. The excessive generation of ROS leads to oxidative stress, which is associated with numerous diseases such as cancer, diabetes, and neurodegenerative disorders. Superoxide ($O_2^{\bullet-}$), hydrogen peroxide (H_2O_2), and hydroxyl radicals (•OH) are the most common ROS involved in a wide range of human diseases. Therefore, sensitive and selective detection of these ROS is of paramount importance for understanding their roles in biological systems and for disease diagnosis. Among the various detection methods, electrochemical techniques have gained significant attention due to their high sensitivity, selectivity, and real-time monitoring capabilities. Electrochemical methods incorporate both organic and inorganic molecules to detect and monitor ROS, facilitating a deeper understanding of how their levels influence diseases linked to oxidative stress. This review aims to provide a critical discussion on the recent advances in electrochemical methods for detecting $O_2^{\bullet-}$, H_2O_2, and •OH. The review also highlights the application of these electrochemical techniques in detecting ROS in living cells and discusses the challenges and future perspectives in this field.

Keywords: reactive oxygen species, electrochemical sensors, enzyme-based biosensors, enzyme-free sensors, oxidative stress

1. Introduction

Reactive oxygen species (ROS), which are believed to be associated with a variety of pathological conditions, have caught the attention of many researchers in medical, biological, and chemical fields. ROS are reactive molecules that can be generated through several mechanisms, including incomplete oxidation of molecular oxygen. ROS primarily refers to free radicals, including hydroxyl (•OH), superoxide ($O_2^{\bullet-}$), peroxynitrite ($ONOO^-$), peroxy radical (ROO•), and alkoxy radical (RO•). Additionally, this group includes non-radical reactive molecules like hydrogen peroxide (H_2O_2) and singlet oxygen ($^1O_2$). The most frequently found ROS are $O_2^{\bullet-}$, H_2O_2, and •OH. These species are predominantly produced in mammals [1, 2], plants [3], and through various natural environmental processes [4]. Endogenously, the mitochondrial respiration process is the main source of ROS production from oxygen. Exogenously, their generation is triggered by exposure to harmful elements, including xenobiotics, pathogens, and ultraviolet light. ROS are commonly found in environments such as natural water sources [5], the smoke from cigarettes [6], and pollutants in the air [7], where they are primarily generated through processes of photolysis and electron transfer. In plants, ROS are generated due to the inevitable release of electrons to O_2 during the electron transport processes of mitochondria, chloroplasts, and plasma membranes or as a side product of diverse metabolic pathways in different cell areas [8-11]. In mammals, the main sources of ROS are nicotinamide adenine dinucleotide phosphate oxidases (NOXs), in conjunction with mitochondrial enzymes that are part of the respiratory chain [12, 13]. Superoxide dismutase (SOD) in the mitochondria is responsible for changing $O_2^{\bullet-}$ into either H_2O_2 or •OH [14]. ROS, at low concentrations, significantly contribute to the regular physiological processes in our bodies [15]. They control the process of transmitting signals, maintaining a stable

internal environment, acting as a defensive mechanism against bacteria, and activating transcription [16].

Nevertheless, an imbalance in the levels of ROS and antioxidants leads to the onset of oxidative stress [17]. Oxidative stress is a condition characterized by an increase in the concentration of ROS inside cells, resulting in harmful effects on DNA, lipids, and proteins [18]. This oxidative stress triggers a variety of medical conditions, such as chronic kidney diseases, diabetes, cancer, neurodegenerative diseases, cardiovascular diseases, chronic obstructive pulmonary diseases (COPD), and plays a significant role in aging [19-23].

Recently, the detection of ROS has attracted more attention in various fields, including biology, medicine, and industry. For instance, in the field of biology, the capability to accurately and promptly detect ROS is pivotal for exploring their dynamic roles and impacts on cellular mechanisms in plants and bacteria [24]. In the medical field, the early detection of variations in ROS levels is crucial for conducting pathological research, diagnosing diseases, and performing health screenings [25]. In the fuel cell industry, monitoring ROS levels is critical for assessing the integrity and efficiency of fuel cells, as it can provide valuable insights into oxidative reactions and material degradation, thereby resulting in improvements in fuel cell design and longevity [26]. However, in the ongoing advancement of ROS detection, several challenges must be addressed. A primary issue is the unique inherent properties of ROS, like their lifespan, diffusion rate, and diverse generation sources. These characteristics can lead to imprecise and inconsistent readings. Additionally, the typically low and unstable concentrations of ROS at their points of origin might make many detection methods inappropriate, particularly in living cells, where precision and reliability are crucial [27].

Researchers have employed various methods to detect ROS, including electron spin resonance [28], immuno-spin trapping [29], mass spectrometry [30], high-performance liquid chromatography (HPLC) [31], chemiluminescence [32], fluorescence spectroscopy [33], spectrophotometry [34], and electrochemical techniques [35]. While each of these techniques offers distinct advantages, some face limitations like the inability to be miniaturized, being labor-intensive, time-consuming, and lacking the capability for on-site analysis [36]. However, among these detection approaches, electrochemical sensing is gaining prominence because of its superior sensitivity, user-friendly operation, miniaturization possibilities, quick reaction time, and cost-effectiveness [35].

Among the different ROS, $O_2^{\bullet-}$, H_2O_2, and •OH are notable for their significant pathological responses. This chapter focuses on the current advancements in electrochemical methods developed to measure these specific ROS.

2. Superoxide ($O_2^{\bullet-}$)

2.1. Introduction to Superoxide ($O_2^{\bullet-}$)

Superoxide ($O_2^{\bullet-}$), a vital molecule in mammalian cells, is produced within mitochondria either through incomplete reduction of oxygen or during adenosine triphosphate (ATP) synthesis. ATP is the primary energy carrier molecule used by cells to power various biological functions. $O_2^{\bullet-}$ serves important functions, acting as a secondary messenger in signaling pathways and regulating gene expression [37]. Although necessary for normal metabolic activities, the levels of $O_2^{\bullet-}$ are regulated by balancing its enzymatic production and degradation by antioxidants. An imbalance leading to excessive $O_2^{\bullet-}$ can induce oxidative stress, damaging nearby proteins and initiating stress-related signaling, which is associated with diseases such as atherosclerosis, autism, Parkinson's, and Alzheimer's [38]. Monitoring $O_2^{\bullet-}$ levels is essential for the early diagnosis of

disease. Normal intracellular $O_2^{\bullet-}$ concentration is around 10-100 nM, but it can increase significantly during stress or illness, up to 0.1 mM [39]. This abnormal increase necessitates the development of detection methods with very low detection thresholds.

Traditional detection methods like ESR, MS, and HPLC have their own drawbacks, especially in detecting $O_2^{\bullet-}$ directly at its generation sources and at lower concentrations. In contrast, electrochemical techniques are increasingly being recognized as more efficient owing to their higher sensitivity and capability to measure $O_2^{\bullet-}$ right at its production sites. Electrochemical techniques are known for their high sensitivity and selectivity, low invasiveness, and quick response, making them ideal for real-time observations in living cells [40]. Nonetheless, further improvements are needed in accuracy, cellular compatibility, and stability, with minimal toxicity.

2.2. Electrochemical Methods for Superoxide ($O_2^{\bullet-}$) Detection

Electrochemical techniques function on the principle of direct interaction between particular sensing element and target molecules. Several studies have reported the detection of $O_2^{\bullet-}$ in various cell types, including tumor cells [41], macrophages [42], cancerous cells [43], skeletal muscle cells [44], and human keratinocyte cells [45]. Despite these advancements, several challenges remain in applying electrochemical techniques for $O_2^{\bullet-}$ detection in biological tissue samples. One of the key challenges in the development of electrochemical methods for detecting $O_2^{\bullet-}$ is ensuring cell penetration. Owing to the fact that $O_2^{\bullet-}$ is produced in the mitochondria and has a limited lifetime due to its high reactivity [46], the electrochemical approach needs to be designed with biological and chemical compatibility to facilitate cell penetration and enable the detection of $O_2^{\bullet-}$ at its point of generation [47]. To enhance the selectivity, sensitivity, and biocompatibility of electrochemical techniques for $O_2^{\bullet-}$ detection in cells and tissues, biological catalysts like superoxide dismutase (SOD) and cytochrome c (Cyt-c) are employed. These

enzymes expedite the dismutation of $O_2^{\bullet-}$, serving as cellular antioxidants [48]. Further sensitivity is achieved by combining these biological molecules with metal oxide nanomaterials, which offer high conductivity and high surface area for attaching biological molecules, thus improving reactive sites and electrical communication with electrodes [49]. Biocompatibility is a critical aspect of electrochemical techniques, necessitating the meticulous choice of nanomaterials and biological molecules combinations. Materials like hydrogel and chitosan are used to coat electrode surfaces, enhancing biocompatibility while preserving the catalytic properties of biological molecules [50]. Even with these enhancements, the fundamental redox reactions between biological molecules and $O_2^{\bullet-}$ remain the same.

A significant drawback of enzyme-based electrochemical sensors is the interference from additional electroactive species at high operating potentials [51]. To overcome this interference, the biological enzymes on the surface of the electrode are often modified with inorganic or organic materials, aiming to lower the operating potential. For example, Crulhas et al. [43] developed a biosensor for detecting $O_2^{\bullet-}$ released from cancer cells by integrating ferrocene (FC) and SOD within a poly (ethylene glycol) diacrylate hydrogel matrix, deposited on gold microelectrodes. This design resulted in a sensitive and selective detection method with a wide linear detection range from 5 to 100 μM and a low limit of detection (LOD) of 0.001 μM [43]. In 2019, Moya et al. modified a platinum electrode with poly (3,4-ethylenedioxythiophene) (PEDOT) and immobilizing SOD by a drop-coating method [52]. This combination aimed to increase sensitivity and specificity in $O_2^{\bullet-}$ detection. The PEDOT layer provided a conducive environment for SOD activity, while ensuring efficient electron transfer. The amperometric biosensor developed through this method exhibited a linear response in the range of 0.175 − 2.8 μM, a high sensitivity of 0.82 μA/μM, and a low LOD of 11.3 nM [52]. Rajesh et al. developed a biosensor for the detection of

$O_2^{\bullet-}$ by integrating carbon nanotubes (CNTs) and polypyrrole (PPy) on a platinum electrode [53]. The CNTs were chosen for their exceptional electrical conductivity and high surface area, enhancing the electron transfer rate. The PPy served as a stable matrix to embed the CNTs and to immobilize the SOD. The electrode surface was first coated with the CNT-PPy composite, creating a conducive environment for SOD attachment. The combination of these materials resulted in a synergistic effect, significantly improving the performance of the biosensor in terms of sensitivity, stability, and response time. This biosensor design enabled the electrochemical detection of $O_2^{\bullet-}$, with a linear detection range from 0.1 to 750 μM and LOD of 0.1 μM [53]. Zhu et al. employed a two-step process to develop an ultrasensitive sensor for detecting $O_2^{\bullet-}$ released from living cells [54]. The first step involved forming a porous copper nanostructure through electrodeposition and hydrogen evolution methods. Subsequently, this structure underwent galvanic replacement to transform into a porous platinum-palladium framework with a high surface area and abundant active sites. SOD was then affixed to this framework. The developed biosensor demonstrated a rapid, specific, and linear amperometric response to $O_2^{\bullet-}$ within the concentration range of 16 μM–1.536 mM, with a detection threshold of 0.13 μM [54]. The capability of the sensor to detect trace amounts of $O_2^{\bullet-}$ from living cells was verified through the detection of $O_2^{\bullet-}$ in living cells induced by Zymosan A, which is known to trigger inflammation responses and $O_2^{\bullet-}$ production.

While this method demonstrated high sensitivity and specificity, the complexity and multi-step nature of their fabrication process could pose challenges for scalability and practical applications. Doran et al. developed a biosensor using a dip-coating approach to immobilize SOD onto a platinum (Pt) electrode modified with poly(phenylenediamine) [55]. To enhance sensitivity and selectivity, they co-immobilized several stabilizers and cross-linkers at various concentrations using a dip-coating approach. The optimally designed sensor used five dip-coatings with a

composite containing 200 U/mL SOD, 0.5% glutaraldehyde, and 2% polyethylenimine. The sensor had a rapid response time of approximately 1 second, high sensitivity of 0.91 nA/μM, and a LOD of 0.063 μM [55]. Although Doran et al. attempted to simplify sensor construction by employing a dip-coating method, their approach introduced its own challenges. The requirement for multiple dip-coating cycles and precise formulation of stabilizers and cross-linkers added complexity and variability to the sensor preparation, potentially limiting its practical applicability. Wang et al. proposed a novel biosensor that simplifies the immobilization process of SOD by using a sodium alginate (SA) sol-gel film to encapsulate and stabilize the enzyme. This approach offers a practical solution that maintains high sensor performance while reducing preparation complexity [56]. The preparation of the modified electrode was relatively straightforward. It involved mixing SOD with SA and applying the mixture to a pretreated gold electrode. The developed sensor demonstrated excellent analytical capabilities including a low operating potential (0V), high selectivity, a broad linear range (0.44 – 229.88 μM), and a low LOD (0.23 μM) [56].

While enzyme-based sensors are capable of reliably detecting $O_2^{\bullet-}$, the enzyme itself encounters many obstacles, including deactivation and inconsistent repeatability of sensor performance in harsh environments [57]. Moreover, the high costs of enzymes, their short lifespan, and reproducibility issues further challenge the practicality of enzyme-based sensors. Their susceptibility to harsh operating conditions intensifies these issues. Natural enzymes, integral to these sensors, are prone to denaturation due to environmental fluctuations in pH, temperature, and humidity. This inherent instability severely restricts the effectiveness of enzyme-based sensors in diverse and demanding applications [58].

In response to these challenges, several innovative technologies including enzyme-free electrochemical sensors have been developed. These sensors stand out for their robust and

consistent performance, capable of accurately detecting analytes even in harsh conditions. Enzyme-free electrochemical sensors employ a variety of materials, which mimic the properties of natural enzymes, for their fabrication. These components include nanotube structures, catalysts, and nanocomposites designed to fabricate sensors that not only mimic enzyme characteristics but also offer robustness and precision [59]. Additionally, synthetic biomimetic enzymes have shown their efficacy as cost-effective artificial enzymes, exhibiting enhanced stability and exceptional recyclability [58, 60].

In 2015, Liu et al. developed an enzyme-free biosensor using Prussian Blue (PB) cubes supported on nitrogen-doped graphene sheets (NGS) for the electrochemical detection of $O_2^{\bullet-}$. The PB-NGS hybrid was synthesized through a facile method and applied to a screen-printed gold electrode (SPGE). They observed a synergistic effect between the PB and NGS, which resulted in boosting the electrochemical performance of the sensor, including enhanced electron transfer from PB to the electrode substrate. The LOD was calculated to be 1.2 μM with a sensitivity of 0.32 $\mu A cm^{-2} \mu M^{-1}$ [60]. Despite its effective catalytic properties, the reliance on PB in the sensor design might introduce stability issues, limiting the reliability and broader application of the sensor. Acknowledging the potential stability issues with PB, in 2017, Liu et al. developed an electrochemical sensor free of enzymes and metals, designed for $O_2^{\bullet-}$ detection through surface interactions with nitrogen-doped hollow mesoporous carbon spheres (N-HMCS). Nitrogen doping was identified as the primary key of high sensitivity, owing to the electron-donating characteristics of nitrogen that enhanced chemical reactivities and electron transport properties. The low detection limit of 2.2 μM could be attributed to various characteristics of N-HMCS, including superior conductivity, abundant pore size, and a large specific surface area of N-HMCS which resulted in enhanced electron transfer during the process of $O_2^{\bullet-}$ reduction [61]. While these enzyme-free

sensors represent a significant advancement in detecting $O_2^{\bullet-}$, their LODs are not sufficiently low to identify $O_2^{\bullet-}$ in living cells, which necessitates nanomolar range detection. Consequently, several electrochemical sensors based on metal oxides have been designed in an effort to increase the sensitivity and selectivity of the sensors.

In 2021, Wang et al. developed a facile method to synthesize ultrathin two-dimensional (2D) graphene-like CeO_2-TiO_2 mesoporous nanosheets (MNS-CeO_2-TiO_2) using polydopamine-coated graphene (rGO@PDA) as a template [62]. The mesoporous nanostructures provided advantages such as enhanced surface roughness, decreased thickness, higher pore volume, and greater specific surface area. In order to obtain a highly efficient electrocatalyst, the composite was also infused with silver nanoparticles (AgNPs). Figure 1 illustrates the fabrication of the final composite (Ag/MNS-CeO_2–TiO_2) which was used to modify screen-printed carbon electrodes (SPCEs) for non-enzymatic electrochemical detection of $O_2^{\bullet-}$. Nafion was drop casted to prevent the detachment of the nanocomposite from the electrode surface. The electrode exhibited a high sensitivity of 737 $\mu Acm^{-2}mM^{-1}$ and a detection limit of 0.0879 μM. In addition, the sensor was successfully applied for real-time monitoring of $O_2^{\bullet-}$ released from HepG2 cells upon stimulation, demonstrating their potential for analysis of $O_2^{\bullet-}$ in biological systems [62]. While the 2D structures offer enhanced surface roughness and electron transfer rates, they may lack the three-dimensional porosity and structural complexity that 3D frameworks provide.

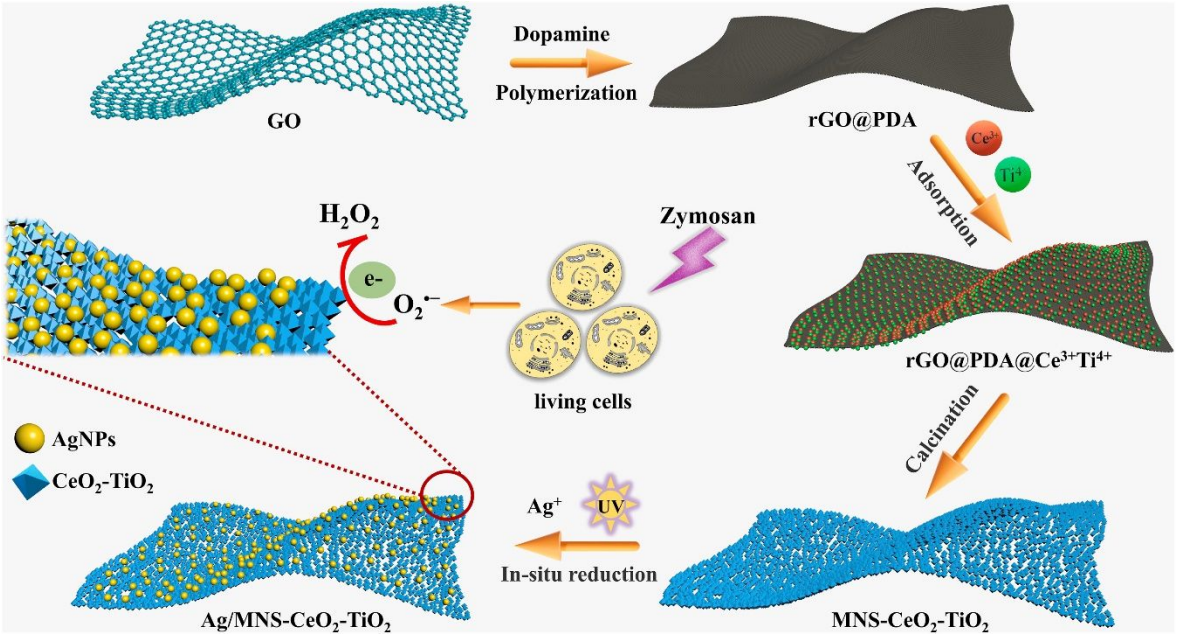

Figure 1. An illustration depicting the fabrication process of Ag/MNS-CeO_2-TiO_2 materials as well as the detection of $O_2^{\bullet-}$ (Reproduced from [62] with permission from ELSEVIER, copyright 2021).

In 2022, Wang et al. developed a novel electrochemical sensor for detecting $O_2^{\bullet-}$ by synthesizing two-dimensional mesoporous nitrogen-rich carbon nanosheets loaded with CeO_2 nanoclusters (2D-mNC@CeO_2) [63]. The synthesis involved a multi-step process where block copolymers served as soft templates while polydopamine was used to chelate metal ions, resulting in an organic-inorganic hybrid material. This hybrid precursor was then transformed into 2D-mNC@CeO_2 through thermal carbonization under inert atmosphere. The resulting material featured a unique structure with uniformly dispersed CeO_2 nanoclusters (<3 nm) on nitrogen-doped carbon nanosheets with hierarchical mesopores. This structure provided enhanced electron transfer, improved mass transport efficiency, and numerous active sites. Additionally, the small size of the CeO_2 nanoclusters resulted in a high Ce^{3+}/Ce^{4+} ratio (43.06%), which improved the superoxide dismutase-like activity of the material. The developed sensor showed excellent performance with a detection limit of 0.179 μM and sensitivity of 401.4 $\mu A cm^{-2} mM^{-1}$. They demonstrated the practical utility of the sensor by successfully monitoring $O_2^{\bullet-}$ released from

$HepG_2$ cells stimulated with Zymosan A, showing its potential for biological applications in clinical diagnostics [63].

In 2020, Cui et al. developed a non-enzymatic electrochemical sensor for $O_2^{\bullet-}$ detection by combining manganese(III) tetraphenyl porphine (MnTPP) as a superoxide dismutase mimic with electrochemically reduced graphene oxide (ERGO) on a GCE [64]. ERGO was first electrodeposited on the electrode surface from a GO dispersion at -1.2 V for 250 s, followed by drop-casting MnTPP aqueous solution to create the MnTPP/ERGO/GCE sensor. The ERGO provided a large surface area for MnTPP immobilization and enhanced conductivity, while MnTPP served as the electrocatalyst for $O_2^{\bullet-}$ reduction. The sensor demonstrated excellent performance with a sensitivity of 445 μA cm^{-2} mM^{-1}, detection limit of 0.039 μM, and a linear range of 0.2-110 μM. They validated the sensor by successfully detecting $O_2^{\bullet-}$ released from MCF-7 breast cancer cells stimulated with zymosan, achieving good selectivity against common interferents and maintaining 93% of its initial response after 4 weeks of storage. This work expanded the application of MnTPP in electroanalytical chemistry while providing a sensitive tool for monitoring $O_2^{\bullet-}$ in biological systems [64].

Using an innovative approach, Gao et al. developed a non-enzymatic electrochemical sensor based on hierarchically porous carbon networks (HPCN) for detecting $O_2^{\bullet-}$ released from living cells [65]. They synthesized HPCN using a dual-step approach combining TMB-induced self-assembly followed by carbonization. The introduction of TMB as a swelling agent during synthesis proved instrumental in generating a distinctive network morphology characterized by an optimized pore distribution hierarchy. The HPCN-modified electrode demonstrated excellent electrochemical performance with high sensitivity (607.4 $\mu A cm^{-2} mM^{-1}$), good selectivity against common interferents, and a detection limit of 0.615 μM. The sensor successfully monitored

dynamic $O_2^{\bullet-}$ released from HepG2 cells upon stimulation. They attributed the superior performance to the hierarchical porous structure of HPCN that facilitated mass transfer and electron transfer efficiency, making it a promising platform for real-time $O_2^{\bullet-}$ detection in biological applications [65].

Hu et al. developed an innovative electrochemical sensor by depositing platinum nanoparticles (PtNPs) on 3D graphene foam (GF), using a substrate-enhanced electroless deposition (SEED) technique (Figure 2) [66]. This 3D GF structure was chosen for its ability to maintain a positive charge interaction with $O_2^{\bullet-}$, enhancing sensor sensitivity. The 3D GF proved advantageous for its biocompatibility, large surface area, and favorable conditions for cell adhesion and growth, which are important for detecting $O_2^{\bullet-}$ directly within cells. The integration of PtNPs with 3D GF not only reduced the repulsion between the electrode surface and the negatively charged $O_2^{\bullet-}$, leading to increased electron transfer and electrocatalytic activity, but also resulted in a distinct and consistent oxidation current in cyclic voltammetry (CV), significantly improving the electrochemical performance with a sensitivity of 1.59 $mAnM^{-1}cm^{-2}$, a detection limit of 10 nM and a swift response time of 3.6 seconds. The study found that 3D PtNPs on graphene foam (Pt@GF) outperformed 2D PtNPs on graphene sheets (Pt@GS) in terms of adsorption capabilities. This 3D setup (Pt@GF) also enhanced the selectivity and sensitivity in detecting $O_2^{\bullet-}$, showing a 140% increase in sensitivity [66]. While this sensor demonstrated excellent analytical properties in $O_2^{\bullet-}$ detection, the synthesis procedure of the composite poses a significant challenge due to the complex preparation processes involved, necessitating a strategy that is both straightforward and effective.

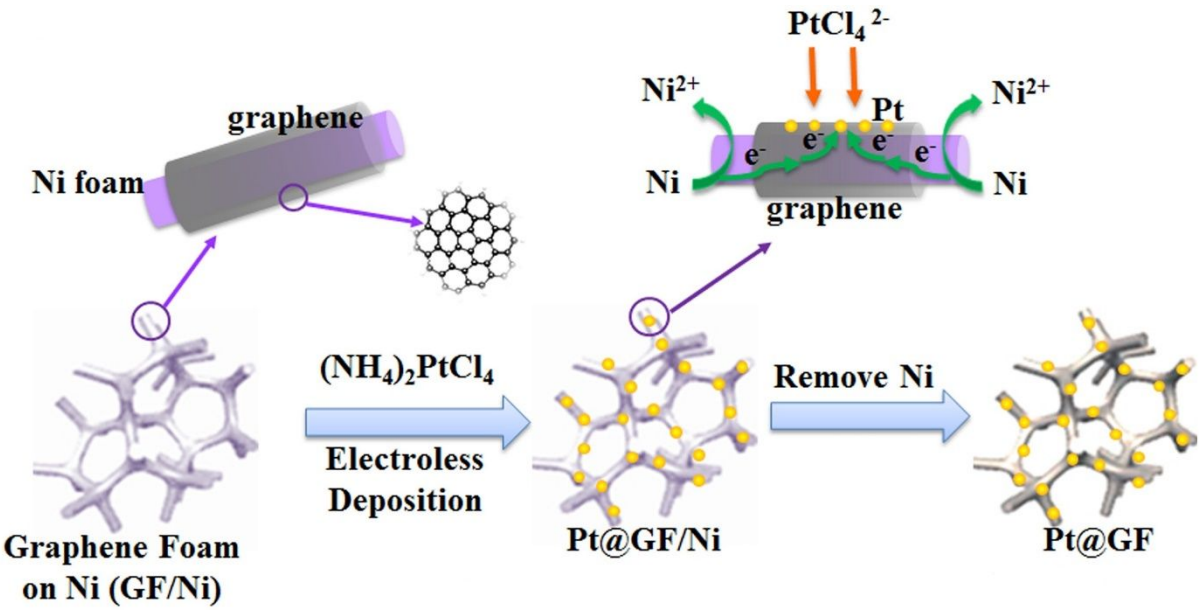

Figure 2. Schematic illustrating the fabrication process of Pt@GF (Reproduced from [66] with permission from ELSEVIER, copyright 2019).

Another example of non-enzymatic sensor for detecting $O_2^{\bullet-}$ was proposed by Liu et al [67]. The sensor was based on AgNPs and L-cysteine functionalized carbon nanotubes (Cys-MWCNTs) nanocomposites. They developed AgNPs/Cys-MWCNTs nanocomposites by uniformly depositing AgNPs on the surface of MWCNTs, which had been functionalized with L-cysteine. This process enhanced the catalytic activity of the resulting composite material. The sensor showed a wide linear range for detecting $O_2^{\bullet-}$, from 7.00×10^{-11} M to 7.41×10^{-5} M, with a remarkably low detection limit of 0.023 nM. These parameters indicate the high sensitivity of the sensor and its capability to detect very low concentrations of $O_2^{\bullet-}$ [67]. A notable limitation of this study is the observed decrease in conductivity, attributed to the quantum size effect of the AgNPs on the Cys-MWCNTs, which could impact the overall efficiency of the sensor in detecting $O_2^{\bullet-}$. According to the Kubo theory, there is an inverse relationship between the size of AgNPs and their conductivity, where smaller nanoparticles experience a stronger quantum size effect and hence poorer conductivity [68]. The application of AgNPs for $O_2^{\bullet-}$ detection has also caught the attention

of other researchers in the field. Wu et al. developed an electrochemical sensor based on AgNPs for detecting $O_2^{\bullet-}$ [69]. They prepared nitrogen-doped cotton carbon fibers (NCFs) using a carbon thermal reduction method. AgNPs were then electro-deposited onto the NCFs. The AgNP/NCF sensor platform designed in this study demonstrated exceptional electrocatalytic performance in its response to $O_2^{\bullet-}$. The sensor demonstrated a remarkable linear response over a vast range spanning 10 orders of magnitude, along with an exceptionally low detection limit of 2.32 fM. Also, its electrochemical sensitivity was notably high, measured at 3.9568 $\mu A \mu M^{-1} cm^{-2}$ [69]. In 2022, Fan et al. developed another silver-based electrochemical sensor for detecting $O_2^{\bullet-}$ released from cancer cells using AgNPs dispersed on a carbon matrix [70]. They synthesized the nanocomposite material by pyrolyzing a silver-based metal-organic framework composed of silver nitrate and benzimidazole ligands at 550 °C. The resulting AgNPs@C material was characterized using SEM, TEM, XRD and other techniques, confirming uniform dispersion of AgNPs (40-50 nm) on the carbon support. The modified glassy carbon electrode (AgNPs@C/GCE) showed excellent electrocatalytic activity toward $O_2^{\bullet-}$ reduction, achieving an ultra-wide linear detection range from 0.3 pM to 57 μM with a detection limit of 101 fM. The sensor demonstrated good selectivity against common interferents and was successfully applied to detect $O_2^{\bullet-}$ released from HeLa cells under both normal conditions and oxidative stress induced by malonic acid. They quantified that individual HeLa cells released $O_2^{\bullet-}$ at a rate of 3.45 $fmolcell^{-1}s^{-1}$ when stimulated with malonic acid. This work provides a sensitive platform for studying cellular oxidative stress through direct electrochemical detection of $O_2^{\bullet-}$ [70].

Exploring beyond AgNPs, researchers have delved into the potential of other nanomaterials to further enhance the detection capabilities of electrochemical sensors for $O_2^{\bullet-}$ detection. For example, Peng et al. developed a novel electrochemical sensor by immobilizing $Mn_3(PO_4)_2$

nanoparticles on magnetic polystyrene nanotubes to modify a magnetic glassy carbon electrode (MGCE) [58]. The $Mn_3(PO_4)_2$ nanoparticles mimicked Mn superoxide dismutase (MnSOD) and acted as the sensing element, while the polystyrene nanotubes functioned as electron carriers and provided a large surface area for $Mn_3(PO_4)_2$ assembly [58]. Their findings demonstrated that the magnetic polystyrene nanotubes, decorated with $Mn_3(PO_4)_2$ nanoparticles, exhibited high catalytic activity in the dismutation of $O_2^{\bullet-}$, leading to a low detection limit of 0.0136 μM without any significant interference.

On a related note, Shen et al. synthesized silica-manganous phosphate (SiO_2-$Mn_3(PO_4)_2$) nanoparticles to mimic Mn-superoxide dismutase (MnSOD) for the detection of $O_2^{\bullet-}$ [71]. The SiO_2-$Mn_3(PO_4)_2$ nanoparticles had numerous benefits, such as a controllable nanoscale shape, a higher specific surface area compared to nano-sheet structures, affordability, a straightforward manufacturing process, and non-toxicity. For the fabrication of the electrochemical sensor, initially, MWCNTs were applied to the electrode surface. Following this step, a portion of SiO_2-$Mn_3(PO_4)_2$ and Nafion mixture was placed onto the MWCNTs-coated. Exhibiting a low detection threshold of 0.0175 μM, the SiO_2-$Mn_3(PO_4)_2$/MWCNTs/GCE sensor effectively detected $O_2^{\bullet-}$ [71].

Building on the concept of $Mn_3(PO_4)_2$-based sensors, Wang et al. developed an innovative approach combining bacterial cellulose and ultrasmall $Mn_3(PO_4)_2$ nanoparticles for real-time detection of $O_2^{\bullet-}$ released from living cells [72]. Using a DNA-mediated assembly strategy, they created a biocompatible sensing platform where $Mn_3(PO_4)_2$ particles were uniformly distributed on bacterial cellulose. The modified screen-printed electrode demonstrated excellent electrocatalytic activity toward $O_2^{\bullet-}$ with a wide linear range from 34.7 nM to 7 μM and a detection limit of 5.87 nM, achieving a sensitivity of 34.1 $\mu A \mu M^{-1} cm^{-2}$. A key innovation was the ability to

grow cells directly on the electrode surface, enabling in situ measurements. When tested with A549 lung cancer cells stimulated by Zymosan A, the electrode with immobilized cells (~28,000 cells) showed rapid response (2.5 s vs 9.0 s for cell suspensions) and generated an average current of 108.3 nA, achieving approximately 1.7-fold higher per-cell sensitivity compared to suspension methods. The enhanced performance was attributed to the minimized diffusion distance between cells and the sensing surface, demonstrating the potential of integrating biocompatible nanomaterials with direct cell measurements for ultrasensitive real-time $O_2^{\bullet-}$ detection [72].

Taking another significant step forward in the development of $Mn_3(PO_4)_2$-based biosensors, Zhao et al. demonstrated a novel approach by creating a flexible 2D/2D heterostructured material combining $Mn_3(PO_4)_2$ and MXene nanosheets [73]. They synthesized 2D $Mn_3(PO_4)_2$ nanosheets with biomimetic enzyme activity and combined them with 2D MXene nanosheets that provided high conductivity and abundant functional groups. The resulting heterostructure, when deposited on polyethylene (PE) film, demonstrated remarkable mechanical flexibility and electrochemical stability during deformation, maintaining its full electrochemical response (100%) even when bent to extreme angles of 180° with a bending radius of 0.75 cm. Furthermore, the material showed exceptional durability by retaining 96% of its original current response after 100 cycles of repeated bending and relaxing, and remarkably maintained over 95% response even after 300 bending cycles. The biosensor achieved impressive performance metrics, including a high sensitivity of 64.93 μA μM^{-1} cm^{-2}, a wide detection range from 5.75 nM to 25.93 μM, and a low detection limit of 1.63 nM. The researchers demonstrated the practical application of the sensor by successfully using it to monitor $O_2^{\bullet-}$ released from human lung cancer cells in real-time under drug stimulation. The enhanced performance was attributed to the surface charge

state promoting $O_2^{\bullet-}$ adsorption and the high-energy active sites improving electrochemical oxidation of $O_2^{\bullet-}$, making this platform promising for studying various biological processes [73].

While modifying electrodes with enzyme mimics has proven effective, ensuring measurement accuracy in complex biological environments remains challenging. To address this limitation, Huang et al. developed a ratiometric electrochemical sensor that provides improved reliability by measuring the ratio of two electrochemical signals - one from the target analyte and another from an internal reference [74]. They synthesized diphenylphosphonate-2-naphthol ester (ND) as a specific recognition molecule that produces electroactive 2-naphthol through nucleophilic substitution with $O_2^{\bullet-}$, while methylene blue (MB) served as the internal reference signal. The sensor was fabricated by co-assembling ND and MB on single-wall carbon nanotube-modified carbon fiber microelectrodes through π-π stacking interactions. This ratiometric design provided excellent selectivity for $O_2^{\bullet-}$ against various potential interferents in the brain and maintained good stability with less than 5.5% signal deviation after 7 days of storage. The sensor demonstrated a linear response range of 2 μM-200 μM with a detection limit of 0.52 μM. They successfully applied the sensor to monitor $O_2^{\bullet-}$ levels in three brain regions (hippocampus, cortex, and striatum) of both normal rats and diabetic model rats under cerebral ischemia conditions, revealing higher $O_2^{\bullet-}$ generation in diabetic rat brains during ischemia compared to normal rats [74].

Cai et al. developed a palm-sized electrochemical sensor system (xenSTAT) integrated with a novel nanozyme-based electrode for detecting cellular $O_2^{\bullet-}$ [75]. They synthesized a manganese phosphate-based nanozyme by self-assembling $Mn_x(PO_4)_y$ monolayer onto porous carbon cubic (PCC) through interactions with melamine and phytic acid. The portable xenSTAT device was designed to connect with smartphones via Bluetooth or computers via USB, enabling

real-time data visualization and customizable detection parameters. The modified electrode exhibited catalytic activity toward $O_2^{\bullet-}$ dismutation through a two-step mechanism involving MnO^{2+} formation. Using CV and chronoamperometry, they achieved a linear detection range for $O_2^{\bullet-}$ with a detection limit of 0.063 μM, showing good selectivity against common interferents like H_2O_2, ascorbic acid, and dopamine. The practical utility of their system was demonstrated by successfully monitoring $O_2^{\bullet-}$ released from Zymosan A-stimulated HeLa cells, suggesting potential applications for in-house diagnosis of $O_2^{\bullet-}$ related diseases [75].

3. Hydrogen Peroxide (H_2O_2)

3.1. Introduction to Hydrogen Peroxide (H_2O_2)

Hydrogen peroxide (H_2O_2), a stable reactive oxygen species (ROS), plays a dual role in cellular processes and can be both beneficial and harmful. H_2O_2 is involved in crucial biological functions such as intercellular signaling and immune response [76]. It stands out among ROS due to its longer lifespan, which enables it to pass through cell membranes and affect cell signaling. However, H_2O_2 concentrations above 100 nM lead to oxidative stress, causing severe diseases including cancer, diabetes, and neurodegenerative disorders [77]. The harmful impact of H_2O_2 stems from its contribution in the formation of hydroxyl radicals (•OH) through the Fenton reaction [78]. Given its role in the development of oxidative stress-related diseases, H_2O_2 has emerged as a crucial subject in the study of oxidative stress. The detection of H_2O_2 has mostly been carried out using techniques such as fluorescence, spectrophotometry, and electrochemistry [79]. In recent years, electrochemical techniques have gained attention for their simplicity, sensitivity, and swift analytical capability, which have made them ideal for H_2O_2 detection.

3.2. Electrochemical Methods for Hydrogen Peroxide (H_2O_2) Detection

H_2O_2 can undergo direct electrochemical oxidation or reduction at conventional solid electrodes. Nevertheless, the efficiency of these methods in analytical applications is limited by poor electrode kinetics and substantial overpotential. These limitations not only diminish the sensing performance but also give rise to significant interferences from other electroactive species present in actual samples, such as bilirubin, urate, ascorbate, etc. [80, 81]. Currently, the primary emphasis of study on H_2O_2 detection is to modify electrodes in order to reduce overpotential and enhance electron transfer kinetics. To perform electrocatalytic H_2O_2 detection, a wide variety of materials including redox proteins, metal oxides, transition metals, metal porphyrins, metal phthalocyanines, carbon nanotubes, dyes, and redox polymers have been used [82]. The discussion in this section focuses on various electrochemical sensors modified with aforementioned materials for the detection of H_2O_2.

Heme proteins, including horseradish peroxidase (HRP), cytochrome c (Cyt c), hemoglobin (Hb), and myoglobin (Mb), are a class of metalloproteins characterized by an iron-centered porphyrin core, which serves as their prosthetic group. Owing to their inherent redox properties, these proteins emerge as promising candidates for bioelectrochemical applications, particularly in the development of biosensors. The most effective method for constructing biosensors involves direct electron transfer between the protein and electrode. This approach provides enhanced selectivity and reduced susceptibility to interfering reactions. However, attaining efficient electron transport between the heme protein and electrode is challenging due to the presence of polypeptides that shield the heme group. This shielding increases the electron transfer distance to such an extent that the tunneling process rarely occurs. A viable solution to

these issues might involve affixing heme-containing proteins onto materials that exhibit high conductivity and offer an extensive surface area.

An increasing number of nanomaterials are being incorporated with heme proteins to develop H_2O_2 sensors based on direct electron transfer due to the advantageous properties of such materials. For example, Wang et al. developed a biosensor based on HRP immobilized on a gold nano-seeds (GNSs) dotted TiO_2 nanocomposite [83]. They used TiO_2 colloids to stabilize the GNSs such that the unique structure of TiO_2 could prevent the GNSs from aggregating. The GNSs–TiO_2 nanocomposite enhanced the electron transfer capacity of HRP and allowed for the preservation of its bioactivity. The HRP enzyme was successfully immobilized in the hybrid film, enabling direct electrochemical activity on glassy carbon electrodes. They employed different techniques like cyclic voltammetry (CV) and amperometry to analyze the electrochemical performance of the biosensor, including its sensitivity and detection limit. This biosensor demonstrated efficient direct electron transfer and enhanced enzymatic electrocatalysis for H_2O_2 detection with a detection limit of 5.9 μM [83]. Xiang et al. developed a zinc oxide (ZnO)-gold nanoparticles (GNPs)-Nafion nanocomposite for HRP immobilization, facilitating direct electron transfer [84]. The ZnO in the nanocomposite provided a large surface area for biomolecule immobilization and had an intrinsic affinity for protein binding, allowing for strong immobilization. On the other hand, GNPs were used for their ability to maintain biocatalytic and electrochemical activity when immobilized on biosensors. However, GNPs tended to aggregate, so they were stabilized within the Nafion polymer in this composite. The nanocomposite enabled direct electron transfer of HRP, as demonstrated through CV. This biosensor exhibited a broad detection range from 15 μM to 1.1 mM, with a detection limit of 9 μM [84]. Another example of using HRP for fabrication of a H_2O_2 biosensor was proposed by Su et al. who developed an

amperometric biosensor using HRP immobilized on amino-functionalized carbon dots (NH_2-CDs) [85]. These NH_2-CDs were synthesized through a hydrothermal method using chitosan and silver nitrate. NH_2-CDs included amino- and carboxyl-groups on their surface, which provided numerous sites for HRP binding. HRP, immobilized on these NH_2-CDs and subsequently deposited on a GCE, effectively retained its bioactivity. This HRP/NH_2-CD modified GCE demonstrated an efficient electrocatalytic reduction of H_2O_2, showing enhanced current response and high sensitivity. The response of the biosensor to H_2O_2 was linear between 5 to 590 nM, with a detection limit of 1.8 nM [85]. Graphene oxide (GO) has also been used for the immobilization of HRP. Wang et al. used HRP and GO co-immobilized on a GCE to develop a biosensor for the detection of H_2O_2 [86]. HRP and GO were co-immobilized on GCE via a simple one-step casting method to form the HRP/GO/GCE biosensor. GO provided a biocompatible interface for HRP immobilization via covalent linkages which helped retain the biological activity of HRP. Additionally, the large surface area of GO increased the loading of HRP while its high conductivity facilitated electron transfer between HRP and the electrode. Furthermore, co-immobilization with GO improved the stability of adsorbed HRP on the electrode surface and preserved the natural conformation of HRP. The biosensor showed satisfactory electrocatalytic reduction of H_2O_2 with a detection limit of 1.6 μM [86].

Cyt c, another heme-based protein, has been used for the fabrication of electrochemical sensors for H_2O_2 detection. Zhang et al. used a composite made of magnetic N-doped carbon nanotubes and AuNPs to immobilize Cyt c. This composite exhibited a large specific surface area, superior electron conductivity, and favorable biocompatibility. Their sensor exhibited enhanced sensitivity, with a LOD as low as 0.3 μM. They found that AuNPs had the ability to maintain the original structure of Cyt c and improve the electrocatalytic properties of Cyt c on the electrode

surface [87]. However, their approach overlooked the orientation of Cyt c, a crucial factor for optimizing its bioelectrocatalytic activity. This oversight left room for Norouz-Sarvestani et al. to enhance the performance of the biosensor further by focusing on the precise orientation of Cyt c. They took advantage of negative surface of Nafion and rGO to create an ideal substrate for immobilizing positively charged Cyt c [88]. The successful orientation of Cyt c ensured effective functioning of Cyt c in the biosensor. In addition, Cyt c exhibited rapid electron transfer kinetics on this modified electrode, enhanced by the mediating effect of graphene. The immobilized Cyt c maintained its electrocatalytic activity, enabling it to catalyze the reduction of H_2O_2 to water. The proposed biosensor exhibited a detection limit as low as 0.4 μM [88].

The use of conductive polymers in fabricating electrochemical sensors represents a notable progress in biosensing research. Aghamiri et al. immobilized Cyt c on an electrode using a polymer-based nanocomposite, hypothesizing that the high electrical conductivity of the nanocomposite would enhance direct electron transfer between the protein and electrode. They introduced a bilayer of polyaniline/polypyrrole (PAN/PPY) as an intermediary layer for this purpose. The mechanical strength of the polymer films was improved by embedding them in carboxylated multi-walled carbon nanotubes (cMWCNTs), leading to improved direct electron transfer and a low detection limit of 0.1 μM [89]. Further innovation was achieved by Akhtar et al. who fabricated a biosensor for detecting H_2O_2 by immobilizing Cyt c onto a 3D porous nickel foam electrode [90]. Here, the Ni foam allowed for facile diffusion of ions and interaction with the immobilized Cyt c, enabling fast electron transfer and rapid sensing of H_2O_2. Cyt c acted as an electron transfer mediator between the active nickel sites on the foam and H_2O_2. The biosensor allowed detection of H_2O_2 over a wide linear range with detection limit of 0.2 M. Due to the

commercial availability and scalability of Ni foam for production, this biosensor offered economic benefits compared to electrodes modified with other nanomaterials.

As stated earlier, other heme proteins, including hemoglobin (Hb), myoglobin, and hemin have the capacity to function as active biological catalysts for the detection of H_2O_2. For example, Ren et al. developed a biosensor based on Hb immobilized on AuNPs trapped in hierarchically porous zeolite MFI for the detection of H_2O_2 [91]. The hierarchically porous zeolite provided large pores for Hb immobilization and interconnected 3D pore networks for efficient mass transfer. AuNPs enhanced conductivity and facilitated direct electron transfer between Hb and the electrode. The resulting biosensor exhibited satisfactory electrocatalytic activity towards H_2O_2 reduction with a wide linear range of 1 μM− 18 mM and a low detection limit of 0.8 μM. Xu et al. [92] further demonstrated the use of Hb in detecting H_2O_2, where they fixed Hb onto a magnetic composite of Fe_3O_4/AuNPs. The goal was to enhance direct electron transfer while keeping the biological activity of Hb intact on the electrode surface. The binding of Hb to Fe_3O_4/AuNPs significantly elevated the overall performance of the sensor, owing to the greater accessibility of redox sites to H_2O_2. They reported a LOD as low as 0.1 μM. Another example was provided by Baghayeri et al. [93], who immobilized Hb on a polypyrrole@poly (styrene-alt-maleic anhydride) covered with 4-aminobenzenesulfonate (PPy@PSMA-g-4ABS) nanocomposite. The PPy@PSMA-g-4ABS nanocomposite provided a suitable microenvironment for Hb immobilization while retaining its natural structure and bioactivity. Direct electron transfer between Hb and the electrode was facilitated by the nanocomposite film. The biosensor had a low detection limit of 0.32 μM for H_2O_2 and fast amperometric response time within 4 s.

Another biosensor based on Hb for the detection of H_2O_2 was proposed by Baghayeri et al. [94] who immobilized Hb on a novel porous nanocomposite of palladium nanoparticles decorated

on iron oxide nanoparticles (Pd@Fe_3O_4) and MWCNTs. The synergistic combination of PdNPs, Fe_3O_4 NPs, and MWCNTs creates a porous nanocomposite with high surface area, conductivity, and biocompatibility, which enabled efficient immobilization and direct electron transfer of Hb for sensitive electrochemical detection of H_2O_2. The biosensor showed excellent electrocatalytic reduction of H_2O_2 with wide linear range of 0.2− 500 μM and low detection limit of 0.063 μM.

As for the use of myoglobin (Mb) for the detection of H_2O_2, Canbay et al. reported the development of a biosensor based on Mb immobilized on a gold electrode modified with cysteamine, MWCNTs, and Nafion [95]. They fabricated the biosensor by first forming a self-assembled monolayer of cysteamine on a gold electrode, followed by immobilization of Mb. Then a composite film of MWCNTs and Nafion was deposited on top to complete the biosensor. The MWCNT-Nafion film helped promote direct electron transfer between the Mb active sites and the electrode, enabling sensitive electrochemical detection. The cysteamine provided improved binding and orientation of the Mb on the surface. The biosensor showed excellent electrocatalytic activity towards the reduction of H_2O_2 with a linear detection range of 0.1− 70 μM and a LOD of 0.01 μM. Similarly, Vilian et al. fabricated a Mb-based biosensor by immobilizing Mb on a GCE modified with a composite of AuNPs, polytyramine (PTy), and MWCNTs [96]. The combination of AuNPs-PTy-MWCNTs nanocomposite and Mb created an optimal microenvironment to retain Mb bioactivity for sensitive detection of H_2O_2. In the presence of H_2O_2, the Mb heme iron center in the ferrous (Fe^{2+}) state gets oxidized to the ferric (Fe^{3+}) state. This oxidized Mb-Fe^{3+} then undergoes reduction at the electrode surface, accepting electrons and reverting to the Mb-Fe^{2+} form. This process of Mb being cyclically oxidized by H_2O_2 and subsequently reduced at the electrode surface produces a measurable redox current signal, allowing for the detection and

quantification of H_2O_2. This biosensor showed excellent electrocatalytic activity towards H_2O_2 reduction with a wide linear range (2 μM – 5mM) and a low detection limit (0.01 μM) [96].

Mesoporous carbon foam (MCF), on the other hand, has been used as a scaffold for the immobilization of Hb, primarily owing to its structural properties. The abundant porosity, high surface area, and superior electronic characteristics of MCF make it an ideal choice for this application. Jahanbakhshi [97] synthesized MCF by a template-free Pechini method and dispersed it in a salep solution to form a stable composite (S-MCF). This composite served as the base for immobilizing Mb, which was then layered onto a GCE (Mb/S-MCF/GCE) to construct the biosensor. The embedded Mb exhibited a reversible redox peak on the S-MCF composite, signifying direct electron transfer to the electrode. This biosensor displayed impressive electrocatalytic activity for reducing H_2O_2, offering a wide linear detection range of 1 − 80 μM and a low detection limit of 0.18 μM. Several other works using Mb for the detection of H_2O_2 have been reported in the literature. For instance, Yoon et al. reported an electrochemical biosensor based on Mb immobilized on a nanocomposite of molybdenum disulfide nanoparticles (MoS_2 NPs) encapsulated within GO sheets [98]. As seen in Figure 3, this nanocomposite was then chemically bonded to a gold electrode. In a subsequent step, Mb was electrostatically bonded to the nanocomposite-modified electrode. This GO@MoS_2 nanocomposite not only provided an ideal surface for Mb immobilization but also enhanced electron transfer, thereby amplifying the electrochemical signals. The resulting Mb/GO@MoS_2 modified gold electrode exhibited outstanding electrocatalytic activity in the reduction of H_2O_2, marked by increased redox peak current. They reported a notably low detection limit, measuring as low as 20 nM [98].

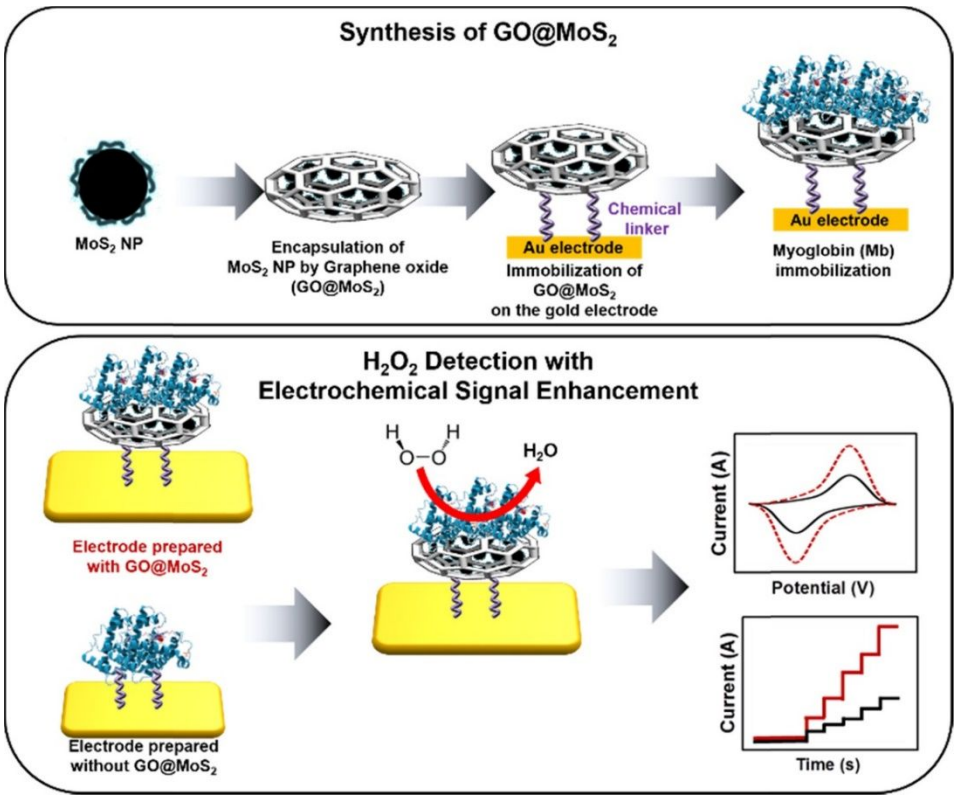

Figure 3. Schematic illustrating the process of preparing GO@MoS_2 for the development of the electrochemical biosensor consisting of Mb and GO@MoS_2 (Reproduced from [98] with permission from ELSEVIER, copyright 2017).

Hemin, known as iron protoporphyrin IX, serves as a crucial cofactor for several key proteins, including cytochrome, hemoglobin, and peroxidase. Its remarkable enzyme-mimicking bioactivity makes it a valuable component in electrochemical sensing applications. However, the catalytic effectiveness of hemin is often impeded due to its self-degradation in water-based environments [99]. Therefore, hemin is commonly stabilized by being anchored to host matrices like metal/metal oxides, zeolites, or carbon-based substances. For example, Le et al. [100] modified an electrode for H_2O_2 detection by combining CNT and thermally reduced GO (TRGO) with hemin (hemin-TRGO-CNT). CNT provided conductivity and a high aspect ratio to proteins, enabling electrolyte ions to diffuse into the electrochemical device, whereas TRGO was capable of facilitating the recognition of biomolecules. The synergy between CNT and TRGO resulted in

a greater surface area and electron transfer between the redox proteins and the electrode, as well as enhanced solubility, dispersibility, and reduced aggregation of the proteins. This could be achieved through the formation of a strong π-π interaction with the protein. The hemin-TRGO-CNT-modified electrode exhibited effective H_2O_2 detection with a LOD of 0.0933 mM [100]. Cao et al. developed an H_2O_2 sensor based on a nitrogen-doped graphene (NGE) and hemin composite material (H-NGE) [101]. They fabricated the composite using a one-pot hydrothermal method. Hemin was anchored onto the NGE sheets during the nitrogen doping process using the reducing agent 2-aminopyridine. Electrochemical tests showed the H-NGE composite had enhanced catalytic activity for the electrochemical reduction of H_2O_2 compared to NGE or hemin alone. This was attributed to the effective immobilization of hemin on NGE and a synergistic effect. The sensor showed a wide range of linearity from 0.2 to 500 mM with a low detection limit of 0.092 mM [101]. Kong et al. further enhanced the sensitivity by incorporating hemin onto a three-dimensional structure composed of GO and single-walled carbon nanotubes (SWCNTs) [102]. The combination of hemin, GO, and SWCNTs resulted in a significant enhancement in the electrochemical performance of the sensor, achieving a low LOD of 0.05 μM. This LOD was lower than what could be achieved with either GO or SWCNTs individually [102]. Recently, the use of porous materials for the immobilization of hemin has emerged as an innovative strategy, offering a new pathway to enhance the stability and functionality of hemin in various applications. For instance, Panagiotopoulos et al. immobilized hemin on mesoporous tin (IV) oxide (SnO_2) films deposited on flexible ITO-PET[1] substrates via a simple hydrothermal method at low temperature. This approach had an advantage of avoiding a complex, time-consuming, and challenging sol-gel process for synthesizing the SnO_2 paste. The SnO_2 film exhibited a high surface area and a

[1] ITO-PET refers to indium tin oxide (ITO) coated poly (ethylene terephthalate) (PET) sheets.

mesoporous structure, allowing high loading of hemin without aggregation. The hemin/SnO_2 sensor demonstrated a linear response from 1.5 to 90 μM and LOD of 1.5 μM [103]. Building on this work, Samourgkanidis et al. [104], immobilized hemin on mesoporous SnO_2 films deposited on Metglas ribbon for a dual-mode sensing of H_2O_2 through electrochemical and magnetoelastic measurements. The key advantage of using Metglas was that it allowed for simultaneous electrochemical and magnetoelastic measurements. While the hemin/SnO_2 film enabled sensitive electrochemical detection of H_2O_2 through its catalytic properties, the magnetoelastic resonance of the Metglas provided an additional sensing mode to quantify mass changes during the reaction. The sensor showed good electrocatalytic activity for H_2O_2 reduction across a linear range of 2− 90 μM with detection limit of 1.6 μM. On the other hand, when H_2O_2 was added to the solution, the hemin/SnO_2-Metglas sensor exhibited a significant decrease in its resonance frequency. This shift in resonance frequency indicated an increase in mass on the sensor surface due to the H_2O_2 reduction reaction.

As stated earlier, an important rationale for incorporating redox proteins into substrates with large surface areas is to enhance both the quantity and stability of redox proteins that are bound to the electrode surface. Metal organic frameworks (MOFs) have emerged as promising materials for immobilizing redox proteins in the fabrication of electrochemical sensors due to their unique properties. MOFs provide high porosity, a large surface area, and tunable pore sizes, allowing for efficient protein immobilization. For example, Wang et al. [105] fabricated an electrochemical sensor using Cu-hemin-MOFs on a chitosan-reduced GO glassy carbon electrode (Cu-hemin-MOFs/CS-rGO@GCE) for detecting H_2O_2 (Figure 4). The CS-rGO enhanced the electrical conductivity and controlled the size/distribution of the Cu-hemin MOFs, while the MOFs structure improved the enzyme-like activity of hemin. Leveraging the advantageous of Cu-MOFs

and CS-rGO, this hemin-based sensor successfully measured H_2O_2 with a low detection limit of 0.019 μM.

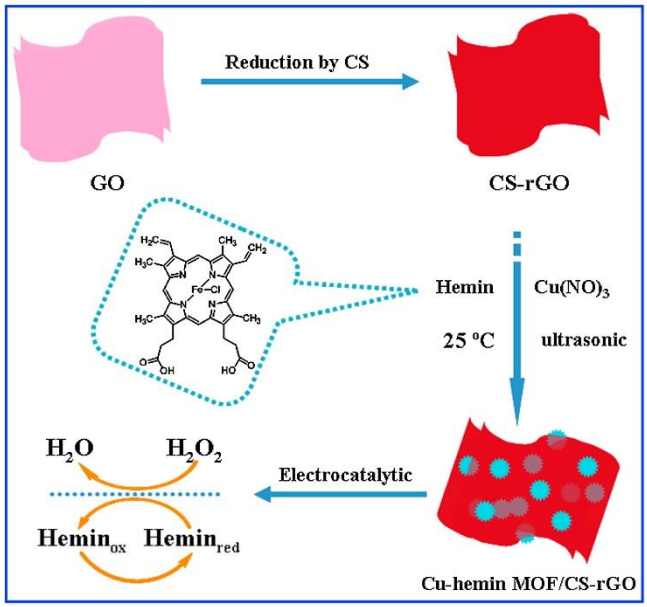

Figure 4. Schematic depicting the fabrication of the Cu-hemin MOFs/CS-rGO nanocomposites and sensing process for H_2O_2 (Reproduced from [105] with permission from ELSEVIER, copyright 2016) .

Another MOFs for immobilizing hemin was proposed by Shu et al. [106] who synthesized nickel metal organic framework (Ni-MOF) nanosheets using a facile hydrothermal method. The Ni-MOFs/hemin nanocomposite-modified electrode exhibited excellent electrocatalytic activity towards H_2O_2 reduction attributed to synergistic effects of Ni-MOFs and hemin. The MOF matrix prevented hemin aggregation and provided high surface area and facilitation of electron transfer kinetics. The sensor exhibited a wide linear detection range from 1 μM to 0.4 mM, and a low detection limit of 0.2 μM.

On a related note, Cheng et al. developed an innovative electrochemical sensor for H_2O_2 detection by integrating three-dimensional flower-like Cu-MOFs with ultra-thin MXene nanosheets [107]. The design incorporates three key advantages: (1) the intrinsic catalytic activity of Cu-containing nanomaterials for H_2O_2 due to the well-matched redox potential of Cu^+/Cu^{2+}

couples, (2) the flower-like Cu-MOFs structure, which provides a high surface area with abundant open metal active sites that enhance H_2O_2 enrichment and subsequent reduction, and (3) the ability of MXene to improve electrical conductivity while offering a large surface area and an electrostatic environment for Cu-MOFs immobilization. The sensor was constructed by first modifying a GCE with MXene, followed by Cu-MOFs deposition. Under optimized conditions, the Cu-MOFs/MXene/GCE sensor exhibited outstanding performance, achieving a wide linear range (1 μM to 6.12 mM) and a low detection limit (0.35 μM). It demonstrated high selectivity against common interferents and successfully detected H_2O_2 in real samples, including milk and serum [107].

In recent years, the use of MOFs in fabricating electrochemical sensors has attracted significant attention. Ghaedamini et al. recently developed a novel non-enzymatic electrochemical biosensor for H_2O_2 detection based on a composite of Ce-MOFs, hemin, and GO [108]. They used Ce-MOFs as a matrix to encapsulate hemin molecules, preventing their self-aggregation, while GO enhanced the conductivity of the sensor. They thoroughly characterized the composite using various techniques including SEM, XRD, FTIR, UV-vis spectroscopy, and TGA, confirming successful integration of the components. The Ce-MOFs@hemin/GO-modified sensor demonstrated excellent electrocatalytic performance toward H_2O_2 reduction, exhibiting a wide linear range from 0.05 Mm to 10 mM with a detection limit of 9.3 μM. The sensor showed high selectivity against common interfering compounds and performed well in complex biological environments, successfully detecting H_2O_2 released from human prostate carcinoma cells and in human serum samples with recovery values between 94.50% and 103.29%. The enhanced performance was attributed to the synergistic effect between Ce-MOFs@hemin and GO, where

Ce-MOFs prevented hemin aggregation and maintained its catalytic activity while GO improved electron transfer [108].

Although the use of redox proteins immobilized on hosted matrices has shown effectiveness in detecting H_2O_2, further thorough study is required to mitigate the degradation of redox proteins in harsh environments. Due to the challenges associated with the application of biological sensing molecules, the focus has shifted towards employing inorganic materials that mimic enzymatic properties. AgNPs have excellent electrocatalytic activity and can promote electron transfer for electrochemical detection of H_2O_2. However, bare AgNPs suffer from aggregation. Several methods have been employed to evenly distribute AgNPs on the electrode surface in order to prevent their aggregation. For example, Wu et al. [109] embedded AgNPs on rGO. The abundant oxygen functional groups on rGO can anchor AgNPs uniformly, thus preventing the aggregation of AgNPs. The AgNPs-rGO modified carbon paste electrode (AgNPs-rGO/CPE) exhibited enhanced electrochemical response and sensitivity for H_2O_2 detection compared to rGO/CPE or plain CPE. Using this sensor, a linear detection range of 1– 1200 μM was obtained with LOD reaching 0.34 μM. In a different approach aimed at preventing the aggregation of AgNPs on electrodes, Goud et al. [110] applied a layer of polyethylene glycol (PEG) and hexamethylenediamine (HMDA) over a SPCE, and then deposited AgNPs on top of it. The primary purpose of the scaffold layer was to regulate the distribution of AgNPs on the electrode surface, leading to reduced clustering, formation of spacious channels that facilitate electron transfer during the deposition of AgNPs, and enhanced accessibility of active sites for reaction with H_2O_2. With a LOD of 1.5 μM, the sensor was used to quantify the H_2O_2 level of a toothpaste product.

The morphology of supporting materials plays a crucial role in determining the electrochemical performance of sensors, as it directly influences the dispersion of active materials, surface area availability, and electron transfer kinetics. Sun et al. studied the performance of AgNPs electrodeposited on different morphologies of zeolitic imidazolate framework-67 (ZIF-67) [111]. They synthesized three types of ZIF-67 structures by varying the solvent: 2D microplates (H-ZIF-67) from water, 2D ultrathin nanosheets (D-ZIF-67) from DMF/water mixture, and 3D rhombic dodecahedron (M-ZIF-67) from methanol. Although 3D structures are often expected to provide superior surface area for nanoparticle dispersion, the 2D H-ZIF-67 demonstrated enhanced performance compared to the 3D M-ZIF-67. This improvement was attributed to higher electrical conductivity and effective prevention of AgNPs aggregation, highlighting that the accessibility and quality of the surface area can be more critical than its total extent in optimizing sensor performance. The optimized sensor exhibited two linear detection ranges (5 mM− 7 mM and 7 mM− 67 mM) and a low detection limit of 1.1 μM. The sensor was successfully applied to detect H_2O_2 released from HepG2 liver cancer cells in real-time, proving its potential for practical biosensing applications. This work highlights how controlling the morphology of supporting materials can enhance electrochemical sensor performance [111].

Expanding on the application of AgNPs for H_2O_2 detection, Zhao et al. dispersed AgNPs over the MoS_2 nanosheets. The AgNPs/MoS_2/GCE exhibited excellent electrocatalytic activity towards the reduction of H_2O_2. The sensor showed improved performance compared to electrodes modified with only AgNPs or MoS_2. This is because MoS_2 has a large specific surface area which allows high loading of AgNPs while preventing their aggregation. Moreover, MoS_2 itself shows electrocatalytic activity towards H_2O_2 reduction. Thus, when combined with the electrocatalytic properties of AgNPs, MoS_2 contributes to a synergistic enhancement in the electrochemical

performance of the sensor. The sensor demonstrated a wide linear response range of 0.025 − 135.2 mM, and a low detection limit of 3.5 μM [112].

Building upon the synergistic properties of MoS_2-based composites, Hu et al. developed a novel electrochemical sensor based on a nanocomposite combining MoS_2 with gold and silver nanoparticles (MoS_2-Au-Ag) [113]. The sensor was constructed by first dispersing MoS_2 in phthalic diglycol diacrylate (PDDA), followed by electrodepositing Au and Ag nanoparticles onto a MoS_2-modified GCE. The MoS_2-Au-Ag/GCE sensor demonstrated excellent electrochemical performance with high sensitivity (405.24 μA mM^{-1} cm^{-2}), a wide linear detection range (0.05 mM- 20 mM), good repeatability (RSD 3.79%), and stability (RSD 3.09%). The sensor was successfully applied to detect H_2O_2 released from living cancer cells (MCF-7) after stimulation with PMA. The biocompatibility of the sensor was confirmed through MTT assays, with cell viability remaining above 90% even at 25 μgmL^{-1} of nanomaterial concentration. This work presents a promising platform for early cancer diagnosis and potential applications in biological and biomedical fields [113].

Copper nanoparticles (CuNPs) have attracted a lot of attention owing to their exceptional catalytic efficacy towards the reduction of H_2O_2. For example, Mani et al. [114] developed a method to electrodeposit CuNPs using pectin as a biopolymer scaffold and graphene nanosheets as the support. They first electrochemically reduced the GO to graphene nanosheets directly on the GCE surface by CV scans. Then, the CuNPs were electrodeposited onto the graphene nanosheets using the biopolymer pectin as a stabilizing scaffold. During electrodeposition, the pectin served as a stabilizing scaffold allowing uniform formation and distribution of CuNPs on the graphene surface. The sensor showed good analytical performance in terms of linear range (1μM− 1 mM), sensitivity (0.391 μAμ$M^{-1}cm^{-2}$) and detection limit (0.35 μM). In another interesting work, Wang

et al. [115] developed a non-enzymatic electrochemical biosensor using copper oxide CuO NPs decorated on black phosphorus nanosheets (BP NSs). BP is a 2D material that provides a large specific surface area to allow high loading and dispersion of the CuO NPs. Moreover, it has excellent electrical conductivity and electron mobility that facilitates rapid electron transfer between the analyte H_2O_2 and the electrode surface. Therefore, synergistic effects between CuO and BP enabled enhanced H_2O_2 adsorption and efficient interfacial electron transfer, contributing to the high sensitivity of the sensor. A wide linear detection range of 0.2– 99.8 μM and a very low detection limit of 30 nM was reported for this sensor. In addition, they applied this sensor successfully to detect pathological H_2O_2 levels in saliva and gingival crevicular fluid samples from periodontitis patients, enabling differentiation from healthy controls.

While monometallic-based electrochemical sensors have demonstrated efficacy in detecting H_2O_2, further enhancements are required in the areas of electrocatalytic activity, conductivity, and sustainability in order to attain superior levels of sensitivity, selectivity, and repeatability. Consequently, bimetallic nanoparticles have drawn attention in recent years due to their remarkable electronic, catalytic, and optical characteristics. The development of electrochemical sensors for the detection of H_2O_2 in biological fluids has been significantly enhanced through the incorporation of bimetallic nanoparticles [116]. Bimetallic nanoparticles have been demonstrated to significantly improve both the electrochemical activity and sensitivity of the sensors. Various combinations of multiple transition metals have been extensively studied and have shown promising advancements in the field of electrochemical sensors. For example, Li et al. [117] developed non-enzymatic electrochemical sensors based on the Au-Pd/MoS_2 nanocomposite modified electrode for the detection of H_2O_2. They synthesized and used MoS_2 nanosheets to support Au-Pd nanoparticles via a thermal co-reduction technique. They took

advantage of the synergistic effects between Au and Pd, where Au provided good conductivity and Pd exhibited superior electrocatalytic activity. On the other hand, the Au-Pd bimetallic nanoparticles generated on the MoS_2 nanosheets were smaller in size compared to individual Au or Pd nanoparticles. The smaller size led to higher surface area and more active sites promoting the electrocatalytic performance. The sensor demonstrated a wide linear range of 0.8 μM– 10 mM and a low detection limit of 0.16 μM. Building upon these advances in bimetallic nanoparticle sensors, Sangkaew et al. developed a highly sensitive non-enzymatic electrochemical sensor for detecting H_2O_2 adulteration in raw cow milk using bimetallic AuPt NPs as electrocatalysts. They synthesized AuPt NPs with different Au:Pt molar ratios and found that Au1Pt2 (1:2 ratio) exhibited optimal electrocatalytic performance for H_2O_2 detection [118]. The sensor was constructed by modifying SPCEs with Au1Pt2 NPs. When tested with ultra-high temperature (UHT) milk samples, the sensor demonstrated good sensitivity (152.9 $\mu AmM^{-1}cm^{-2}$), a low detection limit (4.8 μM), and excellent reproducibility (RSD <4%) with stability up to 4 months. For real-world application, they coupled the sensor with a portable electrochemical analyzer for on-site detection of H_2O_2 in raw cow milk samples, achieving a linear response range of 2.5 μM− 5000 μM with sensitivity of 155.5 $\mu AmM^{-1}cm^{-2}$ and detection limit of 2.5 μM. The enhanced sensing performance was attributed to the synergistic electrocatalytic effect between Au and Pt in the bimetallic nanoparticles. This sensor offers a practical solution for rapid, sensitive, and on-site monitoring of H_2O_2 adulteration in raw milk, outperforming conventional detection methods like commercial test strips [118].

Expanding on the application of PtNPs, Oh et al. developed a flexible and transparent electrochemical sensor for non-enzymatic detection of H_2O_2 released from living cells [119]. The sensor was fabricated by electrodepositing PtNPs onto a SWCNT network on a poly(ethylene

terephthalate) (PET) substrate using CV. The PtNPs/SWCNT/PET sensor demonstrated excellent electrocatalytic activity towards H_2O_2, with a wide dynamic range of 500 nM to 1 M and a low detection limit of 228 nM. The sensor showed good selectivity against common interfering species and maintained stable performance even under various bending angles. The biocompatibility of the sensor was confirmed through successful culture and proliferation of HeLa cells on its surface. Using interdigitated electrode arrays with different patterns, the researchers demonstrated real-time monitoring of H_2O_2 released from HeLa cells under drug stimulation, even in mechanically deformed states. The synergistic combination of PtNPs catalytic activity, SWCNT conductivity, and PET flexibility resulted in a high-performance, flexible sensor, ideal for sensitive H_2O_2 detection in cell-based assays and with strong potential for wearable biosensing applications [119].

Zhao et al. synthesized bimetallic Ag-Au NPs by supporting them on rGO using alginate as both a stabilizer and reductant. The selection of Ag and Au was based on their high biocompatibility, catalytic activity, and straightforward synthesis. Their findings demonstrated that the use of Ag-Au NPs in the electrochemical sensor resulted in superior efficacy in detecting H_2O_2, with a LOD of 0.57 μM. This was attributed to the Ag-Au bimetallic nanoparticles which provided a greater quantity of catalytically active sites compared to the monometallic nanoparticles [120]. Other bimetallic nanomaterials for the detection of H_2O_2 have been reported. For example, in 2021, Hussain et al. reported the development of nickel-cobalt (Ni-Co) bimetallic nanowires (BMNWs) as non-enzymatic electrocatalysts for sensitive detection of H_2O_2 [121]. They synthesized Ni-Co BMNWs with tunable composition by a template-assisted electrodeposition method. They used Ni-Co bimetallic system as it has facile synthesis, controlled morphology, tunable composition and good biocompatibility. The valency states and intrinsic resistivity of Ni and Co can be tuned in the bimetallic system to facilitate charge transfer kinetics, thus improving

the efficiency of electrocatalysis. Ni provides more active sites in the form of Ni^{3+} state which enhances electrocatalytic activity towards H_2O_2. On the other hand, Co provides structural stability to prevent aggregation/degradation of Ni over time and usage. As a result, the Ni-Co coupling offers high conductivity, abundance of active sites, high surface area and excellent electron transfer rate. The sensor showed excellent sensitivity of 2211.4 $\mu AmM^{-1}cm^{-2}$, wide linear detection range of 0.005− 9 mM, low detection limit of 0.5 μM and good reproducibility, stability and selectivity. Also, it was successfully applied for H_2O_2 detection in real samples like milk, contact lens solution, etc. with satisfactory recovery, demonstrating its practical applicability [121].

Several research groups have further fabricated electrochemical sensors for H_2O_2 detection by combining multiple metals. For example, Liu et al. [122] synthesized a nanohybrid material composed of bimetallic palladium-copper (PdCu) nanoparticles supported on carbon black (CB) and modified a GCE with the synthesized PdCu/CB nanohybrid. They found that CB had the ability to maintain the nanostructure of bimetallic PdCu alloy, while also enhancing the dispersion of nanoparticles, as shown in Figure 5A. Additionally, CB offered strong conductivity and a large specific surface area, resulting in a significant enhancement in catalytic efficiency for the reduction of H_2O_2 (Figure 5B) . The sensor showed excellent sensitivity of 1.26 $\mu A\ \mu M^{-1}cm^{-2}$, along with a wide linear detection range from 0.4 μM to 5 mM, low detection limit of 54 nM and good reproducibility and stability.

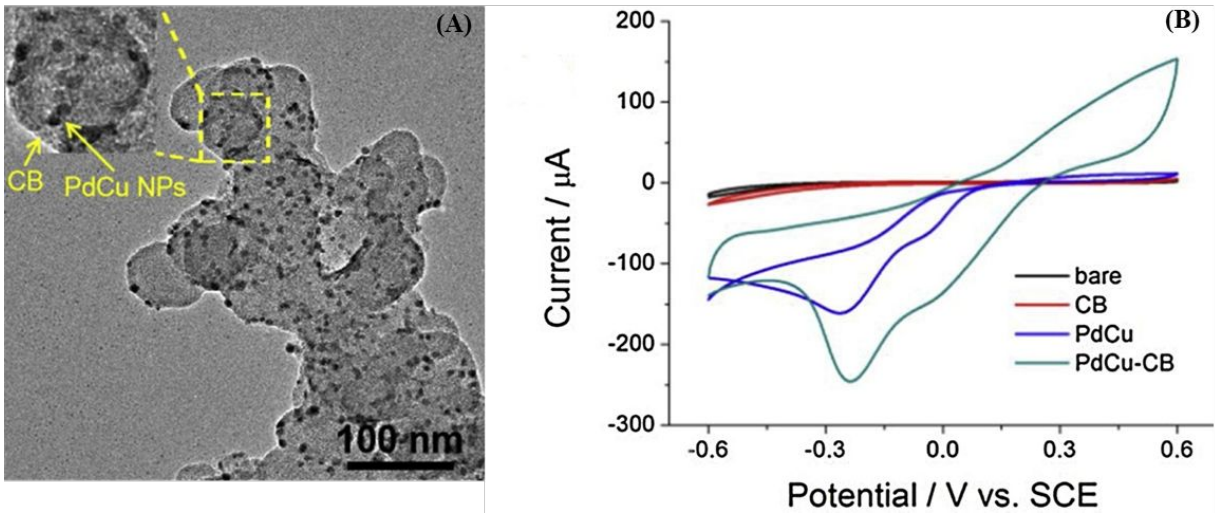

Figure 5. (A) TEM image of PdCu/CB nanohybrid; (B) CVs of the bare GCE, and modified GCE with CB, PdCu and PdCu/CB in the presence of 10 mM H_2O_2 (Reproduced from [122] with permission from ELSEVIER, copyright 2019).

Recently, Sharma et al. introduced a novel non-enzymatic electrochemical sensor for the selective and sensitive detection of H_2O_2 by modifying a GLC with two-dimensional nanoporous magnesium oxide nanosheets (MgO-NSs) [123]. They synthesized MgO-NSs using a straightforward sugar-blowing method, where they simply mixed magnesium nitrate with sucrose in water, dried it, and then heated it to 700°C in a furnace. During heating, the sucrose decomposes and creates gases that form pores in the magnesium oxide structure, resulting in nanosheets with high surface area. The electrochemical sensing capabilities of the MgO-NSs/GCE toward H_2O_2 were investigated using various techniques including CV, DPV, EIS, and amperometry. The fabricated sensor demonstrated excellent analytical performance with a wide linear detection range (20 μM- 1000 μM), low detection limit (0.224 μM), high sensitivity, remarkable selectivity, and good stability. The sensor showed minimal interference from common interfering species and maintained good repeatability (RSD 1.6%) and reproducibility (RSD 1.7%) over 30 days of testing. The practical applicability of the sensor was successfully demonstrated through the detection of H_2O_2 in real milk and mixed-fruit juice samples with excellent recovery rates,

suggesting its potential for various practical applications in food analysis, environmental monitoring, and medical diagnostics [123].

Further enhancement in non-enzymatic electrochemical sensors for H_2O_2 detection was made by Li et al. who developed a sensor based on neuron-network-like copper-doped molybdenum dioxide supported on carbon (Cu-MoO_2/C) nanocomposite [124]. They synthesized Cu-MoO_2/C nanocomposite by pyrolyzing a bimetallic-organic framework precursor. The hierarchical neuron network-like porous morphology of the nanocomposite provided high surface area leading to increased number of electrochemically active sites. The incorporated amorphous carbon also improved electrical conductivity as well as stability of the nanocomposite. A very crucial aspect was the tunable electronic structure and strong interfacial interactions between Cu and MoO_2 which optimized the electrocatalytic activity of the nanocomposite. Compared to MoO_2/C, the Cu-MoO_2/C nanocomposite showed much better sensitivity of 233.4 $mAmM^{-1}cm^{-2}$ and lower detection limit of 85 nM owing to its hierarchical porous structure and synergistic effects of the components. Also, the sensor was successfully applied to detect H_2O_2 content in spiked human serum and commercial disinfectant/contact lens solutions. In another related work, Mani et al. used a carbon cloth (CC) to modify the crystalline structure of nickel cobalt sulfide/cobalt sulfide nanoarrays ($NiCo_2S_4$@CoS_2 NAs), resulting in an incredibly low LOD in the nanomolar range. The key factor behind the excellent electrocatalytic performance of the $NiCo_2S_4$@CoS_2 nanoarrays for H_2O_2 detection lies in the synergistic combination of $NiCo_2S_4$ and CoS_2. $NiCo_2S_4$, a binary transition metal dichalcogenide, possesses outstanding redox properties, mixed valence states that provide enlarged active sites, and high electrical conductivity, making it an efficient electrocatalyst. The combination of $NiCo_2S_4$ with CoS_2 in a core-shell heterostructured nanoarray significantly enhances the electrocatalytic performance. This enhancement is due to the synergistic

effects arising from the close interaction between the two materials. The sensor exhibited the capability to detect H_2O_2 with a LOD as low as 2 nM [125].

Hydrogels have emerged as powerful platforms for biosensing applications due to their three-dimensional porous structure, high surface area, and ability to integrate various functional components. Metal-based hydrogels are particularly interesting as they can combine both structural advantages and catalytic properties, enabling efficient electron transfer and substrate interaction. In 2023, Li et al. developed an innovative dual-detection system for H_2O_2 based on a precisely engineered Pt-Ni hydrogel [126]. The system combined both colorimetric (visual) and electrochemical detection methods. They created a unique dual-structure hydrogel composed of alloyed Pt-Ni nanowires and $Ni(OH)_2$ nanosheets. This structure demonstrated excellent peroxidase-like and electrocatalytic activities, enabling sensitive H_2O_2 detection. The sensor achieved impressive performance metrics, including low detection limits (0.030 μM for colorimetric and 0.15 μM for electrochemical detection), wide linear ranges (0.10 μM- 10.0 mM for colorimetric and 0.50 μM− 5.0 mM for electrochemical), and outstanding long-term stability up to 60 days. Taking the innovation further, the team integrated these detection methods into a portable device using an M5stack development board. For colorimetric detection, they created a test paper system with a color sensor that could quickly process and display results. The electrochemical component was implemented through a custom-designed circuit and screen-printed electrodes. When tested with real biological samples, specifically HeLa cells, the sensors successfully detected H_2O_2 released upon CHAPS[2] stimulation [126].

[2] 3-[(3-cholamidopropyl)dimethylammonio]-1-propanesulfonate

The detection of H_2O_2 released from plant leaves is crucial for understanding stress responses, as H_2O_2 serves as both a stress indicator and a key signaling molecule in plant adaptation mechanisms. Traditional methods for detecting H_2O_2 in plants have limitations including irreversible damage to plant tissues and inability to provide real-time measurements. In 2022, Zhang et al. developed an electrochemical sensor using a multi-walled carbon nanotube-titanium carbide-palladium (MWCNT-$Ti_3C_2T_x$-Pd) nanocomposite, creating a sensitive detection system that can monitor H_2O_2 released from plant leaves in real-time without causing tissue damage [127]. The carbon nanotubes provided excellent conductivity and increased surface area, while $Ti_3C_2T_x$ offered superior electrocatalytic activity, and palladium nanoparticles served as efficient catalysts for H_2O_2 reduction. Their electrochemical detection operated at a remarkably low potential near 0 V, minimizing interference from other biological molecules. For plant stress studies, they devised a simple but effective approach: placing Arabidopsis leaves in phosphate buffer and measuring H_2O_2 release every two hours using differential pulse voltammetry. The sensor demonstrated excellent performance with a linear response range of 0.05 mM− 18 mM and a low detection limit of 3.83 μM. Their sensor overcame these limitations by enabling non-destructive, real-time monitoring of H_2O_2 release. They validated their approach by comparing H_2O_2 measurements between salt-stressed and control Arabidopsis plants, finding elevated H_2O_2 levels in stressed plants that correlated with other physiological stress indicators. The electrochemical sensor showed good stability over 6 days and reproducibility with a relative standard deviation of 6.23% [127].

In 2020, Sun et al. developed a paper-based electrochemical sensor for the rapid and direct detection of H_2O_2 in plant tissues [128]. They modified an indium tin oxide (ITO) working electrode by electroplating gold nanoparticles onto its surface, creating a nano-gold-modified

electrode that enhanced electron transfer and catalytic activity for H_2O_2 reduction. They integrated this electrode into a disposable analytical device and employed differential pulse voltammetry (DPV) to enable direct electrochemical quantification of H_2O_2. To facilitate measurement, they placed small tomato leaf samples (less than 3 mg) directly onto the electrode and added 10 μL of phosphate buffer solution. Their sensor achieved a detection limit of 1 μM, demonstrated a wide linear range, and exhibited strong selectivity against common plant metabolites. They applied this system to monitor H_2O_2 production in *Botrytis cinerea*-infected tomato leaves, effectively capturing dynamic changes over 24 hours. To validate their approach, they compared their electrochemical results with diaminobenzidine (DAB) staining, confirming the accuracy of the sensor for in situ H_2O_2 detection. Their work highlighted the potential of paper-based electrochemical sensors as a rapid, sensitive, and accessible tool for studying H_2O_2 in plant stress responses [128].

Tris(3-hydroxypyridin-4-one) (THP) has traditionally been utilized as a powerful chelating agent, with applications ranging from antibacterial properties to biomedical imaging and catalysis. Its unique molecular structure, featuring three hydroxypyridinone units capable of forming multiple hydrogen bonds, makes it particularly interesting for sensing applications, though this potential has remained largely unexplored in electrochemical detection [129]. Building upon these properties, recently, Failla et al. developed a novel electrochemical sensor for H_2O_2 detection using THP as the sensing material [130]. They synthesized THP and modified SPCEs through a simple drop-casting method. The THP/SPCE sensor demonstrated excellent electrochemical properties with a low LOD of 144 nM, high selectivity against common interferents, good repeatability (RSD = 1.77%), and long-term stability (92% efficiency after 30 days). The sensing mechanism was thoroughly investigated through molecular dynamics simulations, revealing that THP forms

multiple hydrogen bonds with H_2O_2 molecules (average of 15− 16 bonds). The researchers also successfully tested the performance of the sensor in fetal bovine serum (FBS) with recovery values ranging from 94.8% to 104.8%, demonstrating its potential for biological applications. This work represents the first use of THP in electrochemical sensing and offers several advantages including high sensitivity, excellent selectivity, good stability, and cost-effectiveness compared to existing metal-based sensors. The development of this organic molecule-based sensor opens new possibilities for H_2O_2 detection in various fields including healthcare, food safety, and environmental monitoring [130].

4. Hydroxyl Radicals (•OH)

4.1. Introduction to Hydroxyl Radicals (•OH)

Hydroxyl radicals (•OH) are regarded as the most harmful and potentially hazardous ROS generated in biological systems, owing to their capacity to interact with many cellular components and macromolecules [131]. •OH are typically generated through a two-stage process, including the Haber-Weiss (Ⅰ) and the Fenton reaction (Ⅱ). Initially, in the Haber-Weiss reaction, ferric ions are transformed into ferrous ions with the aid of $O_2^{\bullet-}$ molecules. Subsequently, in a reaction known as the Fenton reaction, these ferrous ions interact with H_2O_2, leading to the generation of ferric ions and •OH [131, 132].

$$Fe^{3+} + O_2^{\bullet-} \rightarrow Fe^{2+} + O_2 \quad (Ⅰ)$$

$$Fe^{2+} + H_2O_2 \rightarrow Fe^{3+} + OH^- + \bullet OH \quad (Ⅱ)$$

Due to their extreme reactivity, •OH may react with any biological component, causing significant damage to lipids and proteins via membrane breakdown, protein degradation, and lipid peroxidation (LPO). The oxidation of polyunsaturated fats by •OH can disrupt normal membrane structures through the LPO process [133]. This process is particularly problematic because it generates unstable lipid radicals, which in turn initiate a series of reactions. These reactions result in the creation of fatty acid peroxyl radicals that further propagate cell damage and exacerbate harm to the cell membranes [134]. Due to its detrimental characteristics, •OH have been linked to a variety of diseases, such as cancer, diabetes, liver disease, neurodegenerative disorders, among others [135].

Typical methods for detecting •OH include using spin traps in conjunction with electron paramagnetic resonance (EPR) spectroscopy, along with techniques like chemiluminescence, fluorescence, and electrochemical techniques. Detecting •OH poses significant challenges because of its highly reactive nature and extremely short lifespan. Among these methods, the electrochemical technique has been identified as particularly effective, owing to its high specificity, sensitivity, and its capability for real-time detection of •OH in living cells [136].

4.2. Electrochemical Methods for Hydroxyl Radicals (•OH) Detection

Electrochemical techniques for •OH detection are classified into organic and inorganic methodologies. Organic-based sensors employ a range of materials including conductive polymers, DNA, and organic molecules, whereas inorganic sensors use elements like metal oxide nanoparticles and carbon-based substance [136-141].

The use of DNA as a sensing component was inspired by its susceptibility to direct damage through oxidation reactions with •OH [142]. For example, Huang et al. [143] developed a

biosensor by self-assembling a thiolated DNA aptamer onto a GCE modified with nitrogen-doped porous carbon nanostructures (N-C) and AuNPs. For •OH detection, this aptamer biosensor was immersed in the Fenton reaction to induce oxidative damage to the immobilized DNA by the generated •OH species. The DNA damage was monitored using the electrochemical probe hexaammineruthenium(III) ($[Ru(NH_3)_6]^{3+}$), which binds to the damaged DNA. By measuring the electrochemical signal of surface-bound $[Ru(NH_3)_6]^{3+}$ using square wave voltammetry, they were able to detect and quantify the level of DNA damage and thus the •OH concentration. The biosensor exhibited a wide detection range from 50 to 500 μM, with a LOD of 25 μM. Further, Wu et al. developed an amplified DNA-based electrochemical biosensor for highly sensitive detection of •OH [137]. This group constructed the sensor interface by immobilizing a thiol-modified DNA1. Upon exposure to the Fenton reaction, •OH generated through the reaction induce oxidative damage to the DNA1 layer. They employed an electroactive methylene blue probe to monitor this DNA damage via its intercalative binding affinity that translates damage levels into measurable current signals. To enhance sensitivity, they implemented a biobarcode nanoparticle amplification strategy using AuNPs functionalized with a complementary DNA2 sequence (Figure 6). More residual undamaged DNA1 allows higher loading of DNA2-conjugated AuNPs, further enhancing the redox current signal of methylene blue. This amplified electrochemical biosensor achieved •OH detection over a wide dynamic range from 5 μM to 10 mM, with a detection limit as low as 3 μM. Additionally, this DNA damage principle demonstrates potential for evaluating antioxidants that protect against oxidative damage [144].

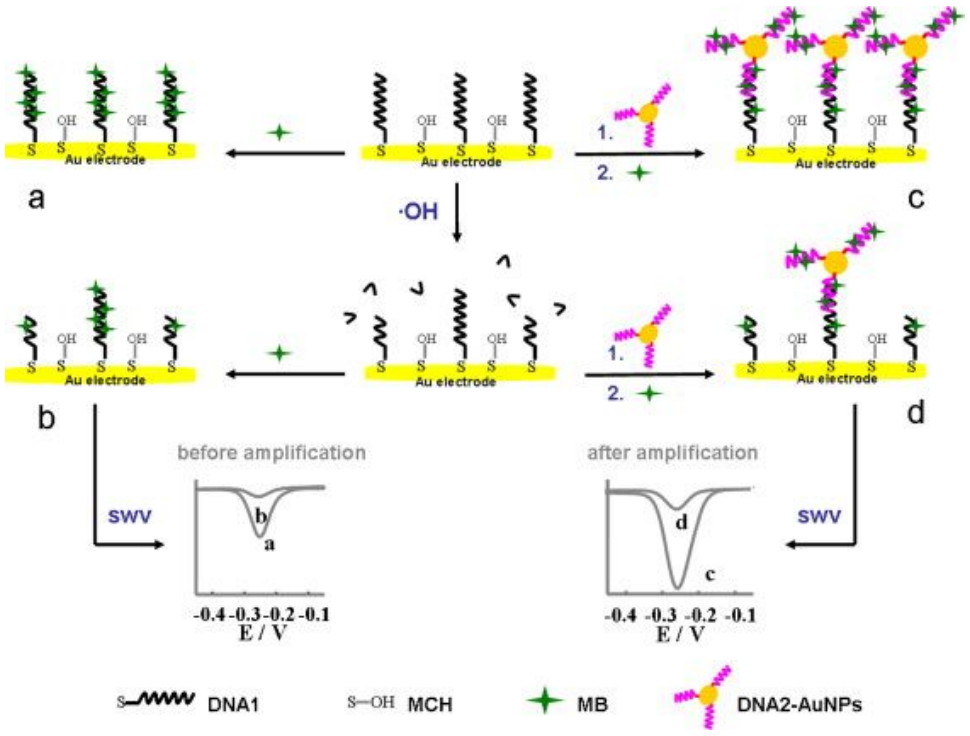

Figure 6. Schematic of the DNA-based electrochemical biosensor for detecting •OH, showing a gold electrode with thiol-modified DNA1 and methylene blue probe, amplified by DNA2-functionalized AuNPs for enhanced sensitivity (Reproduced from [137] with permission from ELSEVIER, copyright 2012).

Abdel-Hamid et al. [145] further investigated the approach of incorporating DNA as the sensing mechanism to detect •OH by studying the antioxidant capabilities of caffeic acid (CAF) in preserving DNA integrity against oxidative damage. This approach was motivated by the role of antioxidants as reducing agents that mitigate damage caused by free radicals. Building on previous research showing the effectiveness of CAF in scavenging free radicals and thus preserving DNA integrity, they modified a GCE with an immobilized double-stranded DNA (dsDNA) layer on MWCNTs. The aim was to investigate the damage of dsDNA by •OH and its protection by CAF. The Fenton reaction was used to generate the damaging •OH. They observed the protective effect of CAF on dsDNA against oxidative harm from •OH, highlighting its free radical scavenging properties.

On a related note, Hájková et al. [146] reported the development of a simple electrochemical biosensor based on a GCE modified with a dsDNA. The dsDNA was adsorbed onto the electrode surface by applying an optimal adsorption potential and allowing electrostatic immobilization. The dsDNA-modified electrode biosensor was used to investigate dsDNA damage induced by •OH generated through three different methods: electrolysis at a boron-doped diamond electrode, the Fenton reaction, and iron(II) autoxidation. They detected the damage using square wave voltammetry to monitor oxidation of DNA bases. They demonstrated that the extent of DNA damage depends on the •OH generation method and conditions like applied current density, iron concentration, and reaction time. The most severe damage occurs with electrogenerated •OH, indicating disruption of nucleobases and phosphodiester bonds in dsDNA. This research group has not provided an explicit explanation for why electrogenerated •OH cause the most severe DNA damage. Nevertheless, it appears that the electrolytic process on the boron-doped diamond electrode surface produces a high flux of •OH close to the DNA biosensor. In contrast, the Fenton reaction and iron autoxidation methods generate •OH at a relatively slower and more diffused rate. Therefore, the high localized concentration and continuous production of •OH through the electrolytic process facilitate rapid and repeated attacks on the immobilized dsDNA before the radicals diffuse away [146].

In addition to DNA-based biosensors, several other organic compounds have also been reported as sensing elements of electrochemical sensors designed for the detection of •OH. Flavonoids, which are polyphenolic compounds found in high quantities in plants, exhibit high reactivity towards highly oxidative species like •OH [147, 148]. This characteristic was harnessed by Jabeen et al. [139], who developed flavonoid-modified electrodes as electrochemical sensors for sensitive and selective detection of •OH. They immobilized flavonoids (morin, quercetin,

primuletin) and their copper and iron complexes on fluorine-doped tin oxide electrodes using amino-silanization chemistry to create a stable sensor coating. Then, by generating •OH using controlled electrolysis on a boron-doped diamond electrode, they noted a linear decline in the flavonoid oxidation peak currents as the concentration of •OH increased. This phenomenon served as the analytical signal necessary for the quantification of •OH [139]. 6-(Ferrocenyl) hexanethiol (6-FcHT) is another organic candidate for the detection of •OH. 6-FcHT can selectively react with •OH leading to changes in its electrochemical oxidation signal. Xu et al. reported the development of a novel electrochemical sensor for the detection of •OH based on a nanoporous gold layer (NPGL) modified gold electrode, onto which 6-FcHT was self-assembled (Figure 7) [149]. The NPGL provided a 3D structure with a large surface area and excellent conductivity, allowing more 6-FcHT to be immobilized on the sensor surface. Using the 6-FcHT/GE directly resulted in a sensitivity of 0.0305 mA nM^{-1} and a LOD of 0.133 nM. This sensitivity notably improved to 0.1364 mA nM^{-1} with an impressive LOD of 0.316 pM following NPGL modification. The efficacy of the sensor was further validated in an in vitro biological system using human liver cancer (HepG2) cell culture solutions, where it successfully detected elevated •OH levels in treated HepG2 cells. Moreover, consistent with expectations, the introduction of antioxidants like ascorbic acid, uric acid, and glutathione resulted in a significant reduction in the electrical current, demonstrating the responsiveness of the sensor to changes in the oxidative environment.

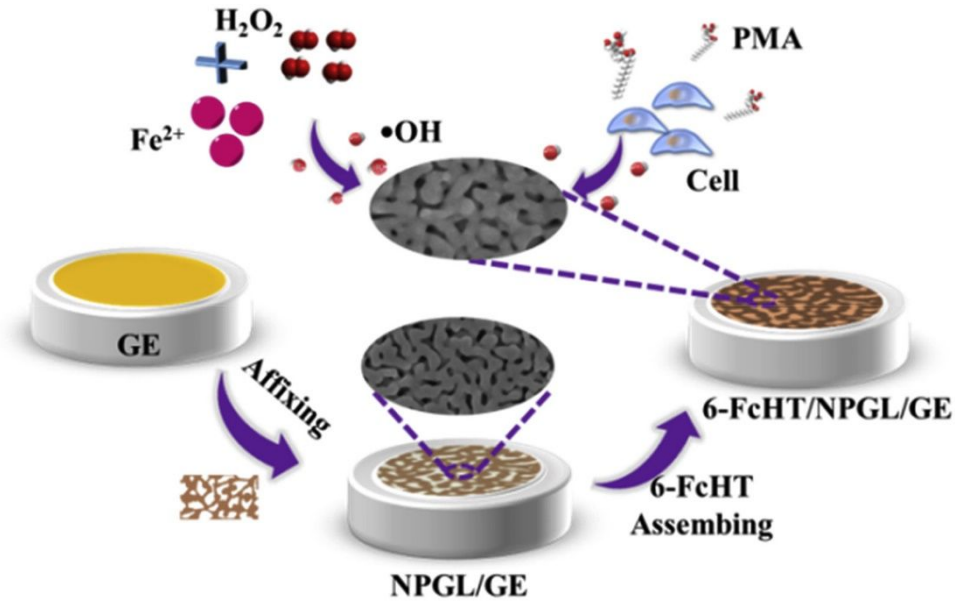

Figure 7. The schematic illustrating the procedure for constructing the 6-FcHT/NPGL/GE (Reproduced from [150] with permission from ELSEVIER, copyright 2020).

In another remarkable work, Ding et al. [151] fabricated a tungsten nanoelectrode by electrochemically etching a tungsten wire to get a sharp tip, then coating it with AuNPs and a self-assembled monolayer of 1-hexanethiol (HAT) (Figure 8). The sharp tip of the tungsten nanoelectrode allowed it to easily penetrate the cell membrane without causing significant damage. They used this nanoelectrode to detect •OH inside living macrophage cells and found higher •OH levels in the cytoplasm compared to the nucleus, and the levels increased upon stimulating oxidative stress. In addition, they used several other ROS, including $O_2^{\bullet-}$, H_2O_2, ClO^- and NO_2^- to assess its selectivity towards •OH. Despite the presence of these ROS at concentrations105-fold higher than •OH, no response was observed for them, underscoring the exceptional selectivity of the sensor towards •OH. Remarkably, they detected increased •OH in an Alzheimer's disease model by treating cells with amyloid beta (Aβ) peptide. Alzheimer's disease involves buildup of Aβ peptide in the brain. Aβ is thought to cause oxidative stress in cells. To model Alzheimer's disease in vitro, this group treated macrophage cells with Aβ peptide, and they were able to detect

a 3.8-fold increase in •OH levels in the cytoplasm of Aβ-treated cells compared to untreated cells. Moreover, they demonstrated that the natural substance cordycepin decreases •OH levels in this model by stimulating antioxidant enzymes, suggesting a possible treatment strategy [151].

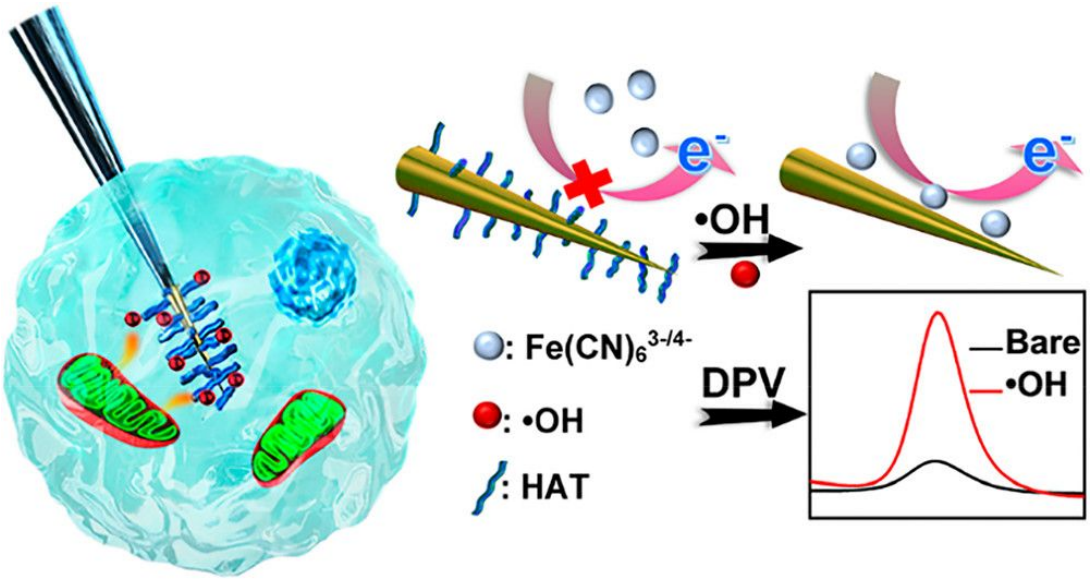

Figure 8. Schematic diagram of the tungsten nanoelectrode modified with HAT used for the detection of •OH at the single-cell level (Reproduced from [151] with permission from ACS, copyright 2020).

Several other organic molecules have been integrated with electrochemical techniques for detecting •OH. For example, reduced glutathione (GSH) has been demonstrated to be a promising organic compound for the detection of •OH. GSH is characterized by its ability to donate electrons and is known for its antioxidant and radical scavenging properties, demonstrating a strong affinity for •OH [152]. In a recent study, Ghaedamini et al. [135] immobilized GSH onto a carbon electrode. They used aryl diazonium salt as an interface agent to create a second layer of GSH on the surface of the electrode. They used CV and EIS to analyze the signals produced from the interaction between GSH on the electrode and •OH. The CV curve of the sensor modified with GSH, when tested in the Fenton reagent, displayed a distinct pair of peaks, indicating the redox interaction between the electrochemical sensor and •OH. This sensor demonstrated a direct linear

correlation between its redox response and the •OH concentration, with a detection limit of 49 μM. On the other hand, following a 1-hour immersion in the Fenton solution, the redox peaks on the CV curve of the GSH-modified electrode vanished. This indicated that the GSH immobilized on the electrode underwent oxidation, transforming into glutathione disulfide (GSSG). Furthermore, this group found that the oxidized GSH surface could be restored to its reduced state by treating it with a solution of glutathione reductase (GR) and nicotinamide adenine dinucleotide phosphate (NADPH), suggesting the potential for its reuse in detecting •OH.

Despite the simplicity of preparing these organic-based biosensors without complex procedures, their usage is constrained to specific conditions because organic compounds can denature under harsh and extreme environments. An alternative method in fabricating organic-based electrochemical sensors involves integrating molecularly imprinted polymers (MIPs) with electrochemical techniques. For instance, Qin et al. [153] developed a molecularly imprinted electrochemical sensor using an rGO/AgNPs composite for selective detection of •OH. They integrated AgNPs with rGO to enhance the electrochemical performance of the sensor due to the high conductivity of AgNPs, porosity suitable for imprinting, and their ability to boost electrochemical signals. By electrodepositing an MIP film using 2,5-DHBA as a template onto the rGO/AgNPs surface, they prepared a sensor that could selectively recognize 2,5-DHBA (Figure 9). By quantifying 2,5-DHBA generated from the reaction between •OH and salicylic acid, this group successfully detected •OH indirectly with high sensitivity. A wide detection range from 0.1 to 100 μM along with a low detection limit of 0.021 μM was achieved. Also, by comparing with HPLC, they validated the accuracy of the sensor for •OH analysis in water samples [153].

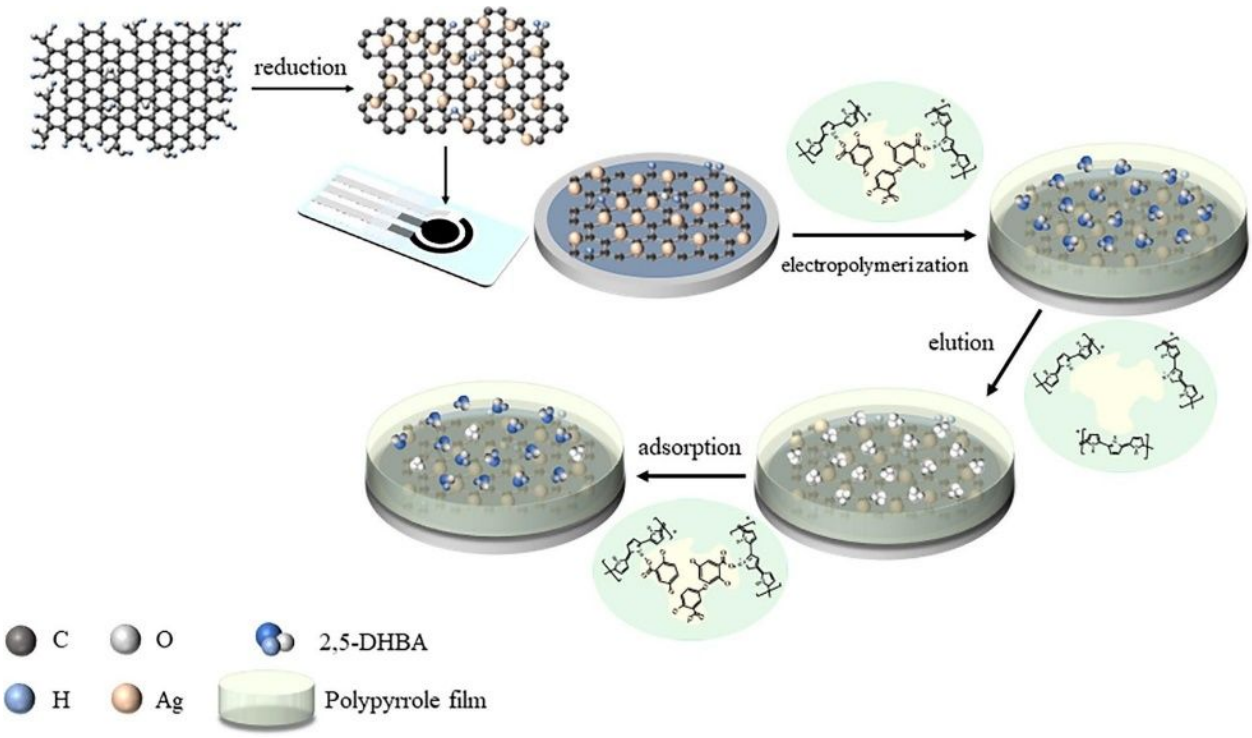

Figure 9. The schematic illustrating the process for the fabrication of MIPs/rGO/AgNPs/SPCE (Reproduced from [153] with permission from ELSEVIER, copyright 2024).

Similarly, Huang et al. [154] developed an electrochemical sensor to detect •OH by measuring the levels of the electroactive substance 2,5-DHBA, which forms from the reaction between •OH and salicylic acid. To achieve this, 2,5-DHBA was electrochemically imprinted in a mixture containing rGO and pyrrole, which was used as a functional monomer. This process created an electrode surface with cavities matching the shape and size of 2,5-DHBA, enabling selective detection. The molecular imprinting technique provided the sensor with specificity, while rGO increased the active sites for imprinting 2,5-DHBA. Notably, they observed that 2,5-DHBA could specifically reattach to the surface cavities on the MIPs/rGO-modified electrochemical sensor, triggering a response proportional to the •OH concentration. This sensor could detect •OH within a linear range from 5.0×10^{-8} to 4.5×10^{-5} M and had a detection limit as low as 2.74 nM.

The specific design of the surface cavities for 2,5-DHBA ensured selective detection of the product resulting from the salicylic acid and •OH reaction [154].

While these electrochemical sensors are suitable for detecting •OH in vitro, they require enhancements for application in intricate biological settings. In such environments, smaller molecules compared to the size of the molecularly imprinted cavities might obstruct these cavities on the electrode surface, consequently diminishing the sensitivity and selectivity of the sensor. Huang et al. [155] developed a novel method for detection of atmospheric •OH using salicylic acid impregnated activated carbon fiber paper (CFP). CFP was activated using a hydrothermal method with sodium citrate to improve its conductivity, hydrophilicity, and binding with salicylic acid. Then, they took activated CFP and spread a solution of salicylic acid evenly onto its surface. As the solution dried, the salicylic acid crystals were left deposited onto and into the pores of the CFP. This allows the CFP to hold a high loading of salicylic acid available to trap atmospheric •OH. When atmospheric •OH reacted with the impregnated salicylic acid, it produced 2,5-DHBA. By quantifying 2,5-DHBA concentration using DPV, they could estimate the atmospheric •OH concentration [155]. In 2020, Huang et al. made further improvements by applying covalent organic frameworks (COFs) to a CFP [156]. This enhancement was intended to increase the absorption of salicylic acid, thereby potentially raising the sensitivity of the sensor for •OH detection. They synthesized a COF material from 1,3,5-triformylphloroglucinol (Tp) and benzidine (BD). This COF(TpBD) was used to modify aminated CFP (CFP-NH_2) via solvothermal synthesis. This modification led to a 1.5-fold increase in the surface area of CFP and improved the hydrophilicity, allowing enhanced loading of salicylic acid. Consequently, there was a notable decrease in the detection limit for •OH (0069 pM), a significant improvement compared to the

unmodified CFP from their earlier study [156]. Figure 10 depicts the COF(TpBD) structure and its utilization in the absorption of salicylic acid and detection of •OH.

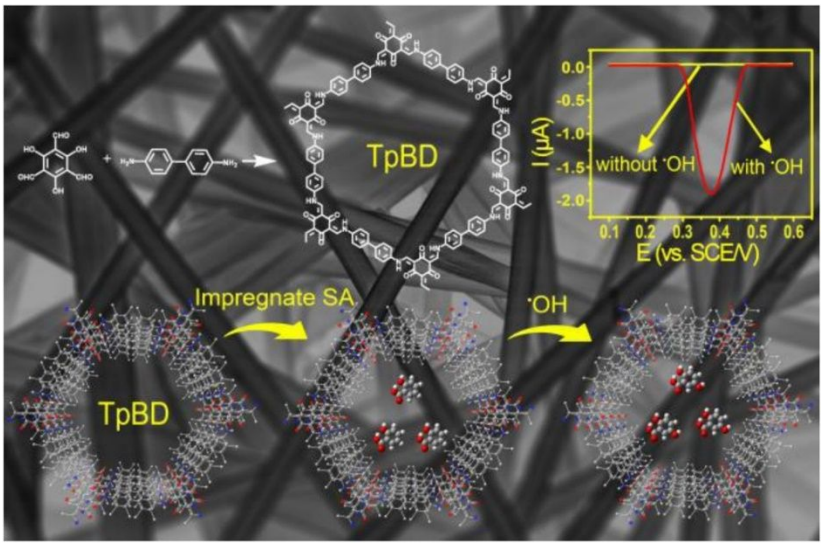

Figure 10. Illustration of COF(TpBD) structure highlighting its use in salicylic acid absorption and •OH detection (Reproduced from [156] with permission from ELSEVIER, copyright 2020).

As mentioned before, employing organic molecules in electrochemical sensors presents several challenges that could potentially be addressed by utilizing inorganic materials. For example, Duanghathaipornsuk et al. [157] developed a composite-based electrochemical sensor using two inorganic layers deposited on a SPCE for the detection of •OH. The first layer of PB was electrochemically deposited to serve as an electrocatalyst, enhancing the sensitivity of the sensor. The second layer, a mixture of cerium oxide nanoparticles (CeNPs) and GO, was applied over the PB layer using a drop-casting method (Figure 11). The CeNPs were chosen for their ability to oscillate between dual oxidation states (Ce^{3+} and Ce^{4+}), with the Ce^{3+} state effectively scavenging •OH. Meanwhile, large surface area of GO and high conductivity significantly boosted the electrical conductivity of the sensor. This sensor demonstrated a linear response to •OH across a concentration spectrum ranging from 0.1 mM to 10 mM, with improved sensitivity when coupled

to the PB catalyst layer. Moreover, the sensor demonstrated an improved LOD of 60 µM in the configuration with the PB layer, compared to a detection limit of 100 µM in the absence of the PB catalyst. However, they found that the PB layer was degraded after being exposed to •OH, causing a reduction in sensor performance [158].

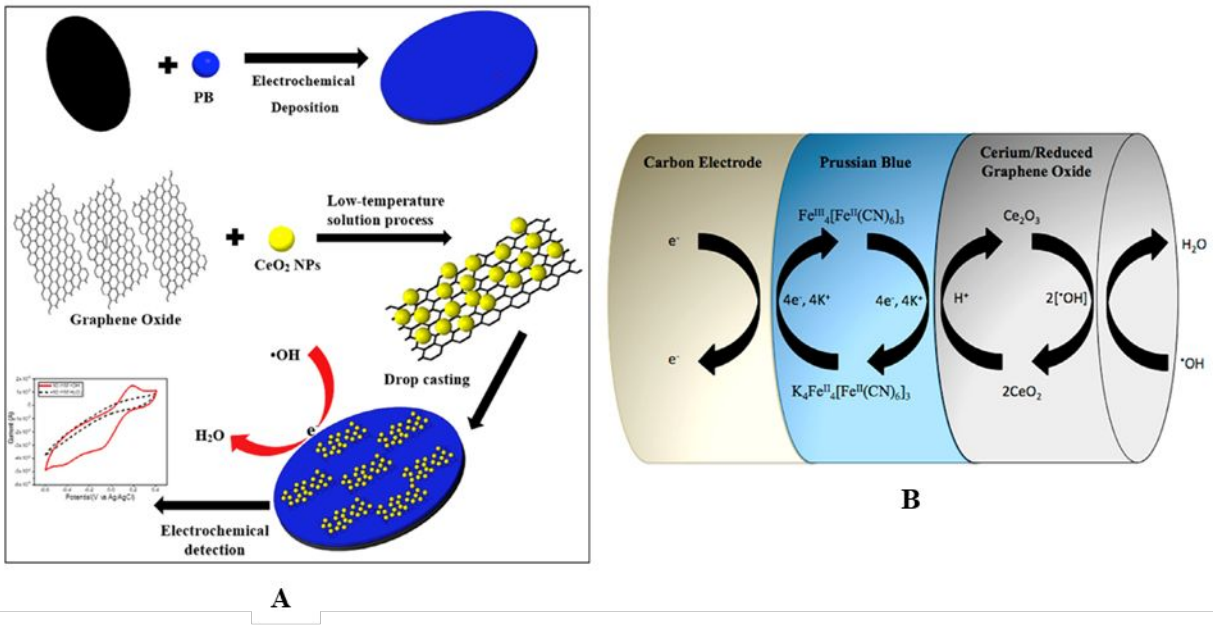

Figure 11. (A) A schematic representation of the fabrication and testing procedures for of the sensor; (B) The •OH detection mechanism (Reproduced from [157] with permission from MDPI, copyright 2020).

Due to the limitations associated with using PB in the development of a reusable electrochemical sensor for •OH detection, Duanghathaipornsuk et al. shifted their focus to examine how variations in particle size and concentration of CeNPs within a CeNPs/GO composite could enhance sensor sensitivity, independently of PB [159]. To do so, they synthesized CeNPs of different sizes (8, 12, 16 nm) and incorporated them with GO in different ratios, varying from a low CeNPs concentration to a high one relative to GO. These varied composites were subsequently deposited onto the SPCEs (Figure 12). The electrochemical sensors based on CeNPs/GO composites exhibited direct correlations between the redox response of the sensor and the

concentration of •OH. Moreover, the capability of the sensor to detect •OH in the Fenton reaction was most efficient when using a composite configuration of 8 nm CeNPs and GO in a 50:50 ratio. For example, the composite containing 50 wt% of 16 nm CeNPs exhibited a LOD of 470 µM for •OH, whereas 50 wt% of 8 nm CeNPs demonstrated a LOD of 85 µM. This enhanced efficiency is attributed to the fact that the number of Ce^{3+} sites and the capacity for •OH scavenging increase as the particle size decreases. Specifically, the smaller 8 nm CeNPs offer a higher surface area to volume ratio compared to their larger 12 and 16 nm counterparts, resulting in more active sites available for reacting with •OH. Additionally, the 50:50 ratio emerged as the most effective balance, as ratios with either too little or too much CeNPs led to a reduction in the number of reactive sites or a decrease in conductivity, respectively [159].

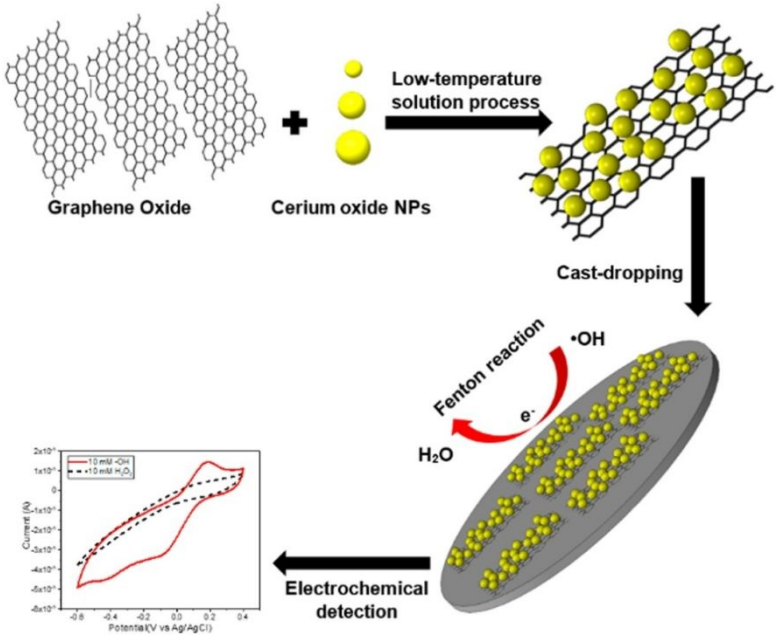

Figure 12. A schematic depicting the fabrication of a CeNPs/GO electrochemical sensor (Reproduced from [159] with permission from ELSEVIER, copyright 2020).

Due to the role of Ce^{3+} sites in the interaction with •OH, several studies have focused on lowering the size of CeNPs in order to increase the quantity of Ce^{3+} sites and enhance their •OH

scavenging capacity [160, 161]. For example, in 2021, Duanghathaipornsuk et al. [160] used surface organometallic chemistry (SOMC) to fabricate nanoscale CeO_x (<2nm) with the aim of increasing the quantity of Ce^{3+} sites for the detection of •OH. The tiny CeO_x nanoclusters provided abundant Ce^{3+} sites to react with and sense •OH via a reversible redox mechanism. They prepared different composites with varying weight percentages (wt%) of CeO_x loading. They found that the 0.64 wt% composite exhibited the best performance for detecting •OH, achieving a notably low LOD of 0.6 μM. This is because at low 0.64 wt% loading, the tiny CeO_x nanoclusters have higher dispersion and less agglomeration on the conductive carbon surface. This maximizes the availability of the reactive Ce^{3+} sites to interact with •OH via the selective redox reaction. Remarkably, the sensor successfully detected in vitro •OH released from mouse preosteoblast cells, with increasing response as oxidative stress was induced.

Inspired by this work, Ghaedamini et al. [162] developed a novel electrochemical sensor using a cerium oxide/gold/carbon nanocomposite for detecting •OH. They initiated a novel approach by first depositing AuNPs on a highly conductive carbon using a deposition-precipitation method. This step was followed by subsequent selective deposition of CeO_x nanoislands on the AuNPs through a controlled surface reaction approach. Their goal was to create tiny clusters of CeO_x that would significantly enhance the electrochemical performance of the sensor. AuNPs were chosen for sensor development due to their exceptional catalytic activity, known for boosting the conductivity of the sensor and thereby increasing its sensitivity. Carbon functioned as a support for the deposition of AuNPs, providing a strong foundation for their attachment. Additionally, it facilitated electron transfer between the electrode and the nanocomposite by providing a conductive matrix. Due to their substantial surface area-to-volume ratio, the AuNPs provided an ample number of active sites to facilitate the distribution of CeO_x domains and hinder their

aggregation. As a result, the combined effects of CeO_x, AuNPs, and carbon significantly enhanced conductivity and electrocatalytic characteristics. The proposed sensor showed two linear detection ranges of 0.05− 0.5 mM and 0.5− 5 mM •OH, with a LOD of 58 μM [162].

Hydrogels, on the other hand, have attracted significant interest because of their distinct porous structure, high surface area, mechanical strength, and favorable biocompatibility [163, 164]. Hydrogels are often used in electrochemical sensing due to their capacity to include nano/bio components and facilitate electrochemical transduction for detecting biological analytes [165]. Polymer-based hydrogels have been investigated for detecting ROS in recent years [140, 166]. For example, Kumar et al. [167] fabricated a sensor using a hybrid alginate-polyacrylamide hydrogel containing rGO-CeO_2 nanocomposite and Cyt c (Figure 13). The porous hydrogel provides a large surface area and hydrated environment to encapsulate Cyt c, while the rGO-CeO_2 nanocomposite enhances conductivity and electrochemical signals. Moreover, a moist environment may support biological processes, boost conductivity, improve sensor signals, and aid in preventing fouling. This sensor showed a low LOD of 0.338 μM, demonstrating the promise of hybrid hydrogels for detecting •OH in real-time.

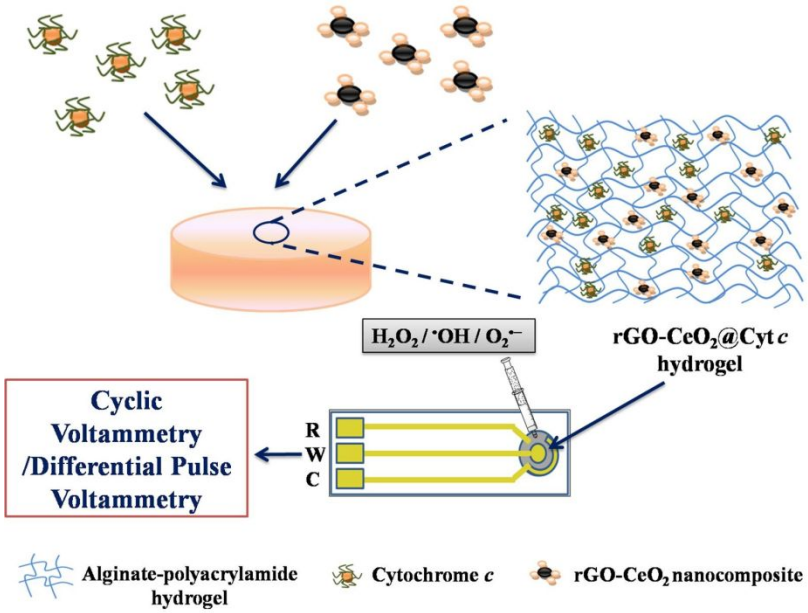

Figure 13. Schematic illustrating the sensing platform based on rGO-CeO_2@Cyt c hydrogel for detecting ROS (Reproduced from [167] with permission from The Royal Society of Chemistry, copyright 2020).

The recent discoveries, along with the development of sensors for detecting ROS at the cellular level, have the potential to benefit the medical community in studying the pharmacological impacts of antioxidant compounds on ROS-related cell damage and in discovering more efficient treatments for the diseases induced by ROS. Table 1 summarizes the major takeaways from this review, highlighting the advantages and disadvantages of different electrochemical methods for ROS detection, including enzyme-based and various non-enzymatic sensor technologies.

Table 1. Summary of electrochemical methods for ROS detection, their advantages and disadvantages

Method	Type	Advantages	Disadvantages	References
Enzyme-based sensors	HRP, SOD, Cyt-c, hemoglobin, myoglobin	High selectivity, biological specificity, low detection limits	Enzyme degradation, short lifespan, high cost	[52] [84] [87] [91] [96]
Non-enzymatic sensors	Nanomaterial-modified electrodes	Stability under harsh conditions, cost-effective, large surface area, improved electron transfer	Potential interference from other electroactive species, lower specificity, possible toxicity	[49] [103] [124]
	MOFs-modified electrodes	High surface area, tunable porosity, enzyme-like catalytic properties	Synthesis complexity, long preparation time	[105-107]
	Bimetallic-modified electrodes	Synergistic catalytic effects, improved sensitivity, high stability	Costly materials, synthesis challenges	[54] [118] [120]
	Graphene and carbon-modified electrodes	High conductivity, biocompatibility, large surface area	Possible aggregation, reproducibility issues	[100-102]

5. Conclusion

The primary sensing components used for detecting ROS are categorized into organic, inorganic, metallic materials. The choice of material should be based on the specific detection conditions. Novel electrochemical techniques have shown satisfactory sensitivity and specificity in detecting ROS in living cells, with varying degrees of advancement depending on the specific kind of ROS. Most of the electrochemical technologies for ROS detection focus on $O_2^{\bullet-}$. The focus on $O_2^{\bullet-}$ is mainly due to its important role as the primary ROS in biological systems. $O_2^{\bullet-}$ is an essential precursor to many other ROS and is present in all living cells; therefore, its detection is crucial for understanding oxidative stress and its effects in a variety of diseases. However, there is

a growing recognition of the importance of detecting other ROS, such as •OH and H_2O_2, due to their distinct biological roles and impacts. •OH, for instance, are highly reactive and can cause immediate damage to DNA, proteins, and lipids, leading to cell death and tissue damage. H_2O_2, on the other hand, is more stable and can diffuse across cell membranes, affecting cells at a distance from its production site. The development of sensors with enhanced selectivity and sensitivity for detecting •OH and H_2O_2 is therefore crucial. These advancements would not only enhance our understanding of the nuanced roles these species play in pathophysiological processes but also improve the detection and monitoring of oxidative stress-related diseases, leading to better diagnostic tools and therapeutic strategies.

Acknowledgements

This material is based upon work supported by the National Science Foundation under Grant No. 1817294 and Grant No. 2141183.

Declaration of competing interest

The authors declare that they have no known competing financial interests or personal relationships that could have appeared to influence the work reported in this paper.

References

1. Koopman, W.J., et al., *Mammalian mitochondrial complex I: biogenesis, regulation, and reactive oxygen species generation.* Antioxidants & redox signaling, 2010. **12**(12): p. 1431-1470.
2. Murphy, M.P., *How mitochondria produce reactive oxygen species.* Biochemical journal, 2009. **417**(1): p. 1-13.
3. Apel, K. and H. Hirt, *Reactive oxygen species: metabolism, oxidative stress, and signaling transduction.* Annual review of plant biology, 2004. **55**: p. 373.
4. Anglada, J.M., et al., *Interconnection of reactive oxygen species chemistry across the interfaces of atmospheric, environmental, and biological processes.* Accounts of chemical research, 2015. **48**(3): p. 575-583.
5. Kieber, D.J., B.M. Peake, and N.M. Scully, *Reactive oxygen species in aquatic ecosystems.* 2003.

6. Church, D.F. and W.A. Pryor, *Free-radical chemistry of cigarette smoke and its toxicological implications.* Environmental health perspectives, 1985. **64**: p. 111-126.
7. Lakey, P.S., et al., *Chemical exposure-response relationship between air pollutants and reactive oxygen species in the human respiratory tract.* Scientific reports, 2016. **6**(1): p. 32916.
8. Foyer, C.H. and J. Harbinson, *Oxygen metabolism and the regulation of photosynthetic electron transport*, in *Causes of photooxidative stress and amelioration of defense systems in plants*. 2019, CRC press. p. 1-42.
9. del Río, L.A., et al., *Reactive oxygen species and reactive nitrogen species in peroxisomes. Production, scavenging, and role in cell signaling.* Plant physiology, 2006. **141**(2): p. 330-335.
10. Blokhina, O. and K.V. Fagerstedt, *Reactive oxygen species and nitric oxide in plant mitochondria: origin and redundant regulatory systems.* Physiologia plantarum, 2010. **138**(4): p. 447-462.
11. Heyno, E., et al., *Oxygen activation at the plasma membrane: relation between superoxide and hydroxyl radical production by isolated membranes.* Planta, 2011. **234**: p. 35-45.
12. Mráček, T., et al., *ROS generation and multiple forms of mammalian mitochondrial glycerol-3-phosphate dehydrogenase.* Biochimica et Biophysica Acta (BBA)-Bioenergetics, 2014. **1837**(1): p. 98-111.
13. Noblanc, A., et al., *Glutathione peroxidases at work on epididymal spermatozoa: an example of the dual effect of reactive oxygen species on mammalian male fertilizing ability.* Journal of andrology, 2011. **32**(6): p. 641-650.
14. Chen, X., et al., *Recent progress in the development of fluorescent, luminescent and colorimetric probes for detection of reactive oxygen and nitrogen species.* Chemical Society Reviews, 2016. **45**(10): p. 2976-3016.
15. Di Meo, S., et al., *Role of ROS and RNS sources in physiological and pathological conditions.* Oxidative medicine and cellular longevity, 2016. **2016**.
16. Reczek, C.R. and N.S. Chandel, *ROS-dependent signal transduction.* Current opinion in cell biology, 2015. **33**: p. 8-13.
17. Morena, M., et al., *Overproduction of reactive oxygen species in end-stage renal disease patients: a potential component of hemodialysis-associated inflammation.* Hemodialysis international, 2005. **9**(1): p. 37-46.
18. Yoshikawa, T. and Y. Naito, *What is oxidative stress?* Japan medical association journal, 2002. **45**(7): p. 271-276.
19. Irazabal, M.V. and V.E. Torres, *Reactive oxygen species and redox signaling in chronic kidney disease.* Cells, 2020. **9**(6): p. 1342.
20. Newsholme, P., et al., *Molecular mechanisms of ROS production and oxidative stress in diabetes.* Biochemical Journal, 2016. **473**(24): p. 4527-4550.
21. Liou, G.-Y. and P. Storz, *Reactive oxygen species in cancer.* Free radical research, 2010. **44**(5): p. 479-496.
22. Afanas' ev, I., *ROS and RNS signaling in heart disorders: could antioxidant treatment be successful?* Oxidative medicine and cellular longevity, 2011. **2011**.
23. Boukhenouna, S., et al., *Reactive oxygen species in chronic obstructive pulmonary disease.* Oxidative medicine and cellular longevity, 2018. **2018**.
24. Akter, S., et al., *Measuring ROS and redox markers in plant cells.* RSC chemical biology, 2021. **2**(5): p. 1384-1401.
25. Li, R., Z. Jia, and M.A. Trush, *Defining ROS in biology and medicine.* Reactive oxygen species (Apex, NC), 2016. **1**(1): p. 9.
26. Frühwirt, P., et al., *Holistic approach to chemical degradation of Nafion membranes in fuel cells: modelling and predictions.* Physical Chemistry Chemical Physics, 2020. **22**(10): p. 5647-5666.

27. Kalyanaraman, B., et al., *Recent developments in detection of superoxide radical anion and hydrogen peroxide: Opportunities, challenges, and implications in redox signaling.* Archives of biochemistry and biophysics, 2017. **617**: p. 38-47.
28. D'Errico, G., et al., *Electron Spin Resonance (ESR) for the study of Reactive Oxygen Species (ROS) on the isolated frog skin (Pelophylax bergeri): A non-invasive method for environmental monitoring.* Environmental Research, 2018. **165**: p. 11-18.
29. Towner, R.A. and N. Smith, *In vivo and in situ detection of macromolecular free radicals using immuno-spin trapping and molecular magnetic resonance imaging.* Antioxidants & redox signaling, 2018. **28**(15): p. 1404-1415.
30. McDonagh, B., *Detection of ROS induced proteomic signatures by mass spectrometry.* Frontiers in physiology, 2017. **8**: p. 470.
31. Zhao, H., et al., *Detection and characterization of the product of hydroethidine and intracellular superoxide by HPLC and limitations of fluorescence.* Proceedings of the National Academy of Sciences, 2005. **102**(16): p. 5727-5732.
32. Yu, W. and L. Zhao, *Chemiluminescence detection of reactive oxygen species generation and potential environmental applications.* TrAC Trends in Analytical Chemistry, 2021. **136**: p. 116197.
33. Nazarewicz, R.R., A. Bikineyeva, and S.I. Dikalov, *Rapid and specific measurements of superoxide using fluorescence spectroscopy.* Journal of biomolecular screening, 2013. **18**(4): p. 498-503.
34. Bartosz, G., *Use of spectroscopic probes for detection of reactive oxygen species.* Clinica Chimica Acta, 2006. **368**(1-2): p. 53-76.
35. Yuasa, M. and K. Oyaizu, *Electrochemical detection and sensing of reactive oxygen species.* Current Organic Chemistry, 2005. **9**(16): p. 1685-1697.
36. Mahato, K., P.K. Maurya, and P. Chandra, *Fundamentals and commercial aspects of nanobiosensors in point-of-care clinical diagnostics.* 3 Biotech, 2018. **8**: p. 1-14.
37. Grivennikova, V.G. and A.D. Vinogradov, *Generation of superoxide by the mitochondrial Complex I.* Biochimica et Biophysica Acta (BBA)-Bioenergetics, 2006. **1757**(5-6): p. 553-561.
38. Manoharan, S., et al., *The role of reactive oxygen species in the pathogenesis of Alzheimer's disease, Parkinson's disease, and Huntington's disease: a mini review.* Oxidative medicine and cellular longevity, 2016. **2016**.
39. Qu, L.-L., et al., *Selective and sensitive detection of intracellular O2•–using Au NPs/Cytochrome c as SERS nanosensors.* Analytical chemistry, 2013. **85**(20): p. 9549-9555.
40. Li, Y., et al., *Electrochemical detection of superoxide anions in HeLa cells by using two enzyme-free sensors prepared from ZIF-8-derived carbon nanomaterials.* Microchimica Acta, 2019. **186**: p. 1-8.
41. Liu, X., et al., *Sensitive detection of superoxide anion released from living cells using silver nanoparticles and functionalized multiwalled carbon nanotube composite.* Sensors and Actuators B: Chemical, 2017. **252**: p. 503-510.
42. Jeong, J., et al., *Ultrasensitive detection of hazardous reactive oxygen species using flexible organic transistors with polyphenol-embedded conjugated polymer sensing layers.* Journal of hazardous materials, 2018. **355**: p. 17-24.
43. Crulhas, B.P., et al., *A novel superoxide anion biosensor for monitoring reactive species of oxygen released by cancer cells.* Electroanalysis, 2017. **29**(5): p. 1252-1257.
44. Sadeghian, R.B., et al., *Online monitoring of superoxide anions released from skeletal muscle cells using an electrochemical biosensor based on thick-film nanoporous gold.* ACS sensors, 2016. **1**(7): p. 921-928.
45. Santharaman, P., et al., *Label-free electrochemical immunosensor for the rapid and sensitive detection of the oxidative stress marker superoxide dismutase 1 at the point-of-care.* Sensors and Actuators B: Chemical, 2016. **236**: p. 546-553.

46. Peshavariya, H.M., G.J. Dusting, and S. Selemidis, *Analysis of dihydroethidium fluorescence for the detection of intracellular and extracellular superoxide produced by NADPH oxidase.* Free radical research, 2007. **41**(6): p. 699-712.
47. Feron, K., et al., *Organic bioelectronics: materials and biocompatibility.* International journal of molecular sciences, 2018. **19**(8): p. 2382.
48. Chen, X.J., et al., *Detection of the superoxide radical anion using various alkanethiol monolayers and immobilized cytochrome c.* Analytical chemistry, 2008. **80**(24): p. 9622-9629.
49. Wang, L., et al., *A novel amperometric biosensor for superoxide anion based on superoxide dismutase immobilized on gold nanoparticle-chitosan-ionic liquid biocomposite film.* Analytica chimica acta, 2013. **758**: p. 66-71.
50. Wang, Y., et al., *Constructing high effective nano-Mn3 (PO4) 2-chitosan in situ electrochemical detection interface for superoxide anions released from living cell.* Biosensors and Bioelectronics, 2019. **133**: p. 133-140.
51. Ghaedamini, H., et al., *A novel ACE2-Based electrochemical biosensor for sensitive detection of SARS-CoV-2.* Anal Biochem, 2024. **689**: p. 115504.
52. Moya, P.M.O., et al., *PEDOT/Superoxide dismutase electrode surface modification for superoxide bioelectrochemical sensing.* Electroanalysis, 2020. **32**(1): p. 29-36.
53. Rajesh, S., et al., *Simultaneous electrochemical determination of superoxide anion radical and nitrite using Cu, ZnSOD immobilized on carbon nanotube in polypyrrole matrix.* Biosensors and Bioelectronics, 2010. **26**(2): p. 689-695.
54. Zhu, X., et al., *Ultrasensitive detection of superoxide anion released from living cells using a porous Pt–Pd decorated enzymatic sensor.* Biosensors and Bioelectronics, 2016. **79**: p. 449-456.
55. Doran, M.M., N.J. Finnerty, and J.P. Lowry, *In–Vitro Development and Characterisation of a Superoxide Dismutase-Based Biosensor.* ChemistrySelect, 2017. **2**(14): p. 4157-4164.
56. Wang, X., et al., *A superoxide anion biosensor based on direct electron transfer of superoxide dismutase on sodium alginate sol–gel film and its application to monitoring of living cells.* Analytica chimica acta, 2012. **717**: p. 61-66.
57. Wang, M.-Q., et al., *Nanostructured cobalt phosphates as excellent biomimetic enzymes to sensitively detect superoxide anions released from living cells.* Biosensors and Bioelectronics, 2017. **87**: p. 998-1004.
58. Peng, F., et al., *Novel biomimetic enzyme for sensitive detection of superoxide anions.* Talanta, 2017. **174**: p. 82-91.
59. Chen, X., et al., *Advances in enzyme-free electrochemical sensors for hydrogen peroxide, glucose, and uric acid.* Microchimica Acta, 2014. **181**: p. 689-705.
60. Liu, T., et al., *Electrocatalytic analysis of superoxide anion radical using nitrogen-doped graphene supported Prussian Blue as a biomimetic superoxide dismutase.* Electrochimica Acta, 2015. **176**: p. 1280-1287.
61. Liu, L., et al., *Enzyme-and metal-free electrochemical sensor for highly sensitive superoxide anion detection based on nitrogen doped hollow mesoporous carbon spheres.* Electrochimica Acta, 2017. **227**: p. 69-76.
62. Wang, Z., et al., *Facile synthesis of ultrathin two-dimensional graphene-like CeO2–TiO2 mesoporous nanosheet loaded with Ag nanoparticles for non-enzymatic electrochemical detection of superoxide anions in HepG2 cells.* Biosensors and Bioelectronics, 2021. **184**: p. 113236.
63. Wang, Z., et al., *Two-dimensional mesoporous nitrogen-rich carbon nanosheets loaded with CeO2 nanoclusters as nanozymes for the electrochemical detection of superoxide anions in HepG2 cells.* Biosensors and Bioelectronics, 2022. **209**: p. 114229.

64. Cui, M., et al., *Electrochemical detection of superoxide anion released by living cells by manganese (III) tetraphenyl porphine as superoxide dismutase mimic.* Chemical Research in Chinese Universities, 2020. **36**(5): p. 774-780.
65. Gao, Q., et al., *Fabrication of hierarchically porous carbon networks for the electrochemical determination of superoxide anion released from living cells.* Sensors and Actuators B: Chemical, 2021. **330**: p. 129309.
66. Hu, F.X., et al., *3D Pt/Graphene foam bioplatform for highly sensitive and selective in-situ adsorption and detection of superoxide anions released from living cells.* Sensors and Actuators B: Chemical, 2019. **287**: p. 209-217.
67. Liu, Y., et al., *Construction of a highly sensitive non-enzymatic sensor for superoxide anion radical detection from living cells.* Biosens Bioelectron, 2017. **90**: p. 39-45.
68. Li, X., et al., *A novel nonenzymatic hydrogen peroxide sensor based on silver nanoparticles and ionic liquid functionalized multiwalled carbon nanotube composite modified electrode.* Electrochimica Acta, 2013. **113**: p. 170-175.
69. Wu, T., et al., *An ultrasensitive electrochemical sensor based on cotton carbon fiber composites for the determination of superoxide anion release from cells.* Microchimica Acta, 2019. **186**: p. 1-9.
70. Fan, W., et al., *Development of a Novel Silver-based Sensing Platform for Detecting Superoxide Anion Released from HeLa Cells Directly.* Electroanalysis, 2022. **34**(6): p. 987-994.
71. Shen, X., et al., *Manganese Phosphate Self-assembled Nanoparticle Surface and Its application for Superoxide Anion Detection.* Sci Rep, 2016. **6**(1): p. 28989.
72. Wang, Y., et al., *BC@ DNA-Mn3 (PO4) 2 nanozyme for real-time detection of superoxide from living cells.* Analytical Chemistry, 2020. **92**(24): p. 15927-15935.
73. Zhao, S.F., et al., *2-D/2-D heterostructured biomimetic enzyme by interfacial assembling Mn 3 (PO 4) 2 and MXene as a flexible platform for realtime sensitive sensing cell superoxide.* Nano Research, 2021. **14**: p. 879-886.
74. Huang, S., et al., *Nonenzymatic electrochemical sensor with ratiometric signal output for selective determination of superoxide anion in rat brain.* Analytical chemistry, 2021. **93**(13): p. 5570-5576.
75. Cai, X., et al., *Smartphone-coupled Electrochemical Analysis of Cellular Superoxide Anions Based on Mnx (PO4) y Monolayer Modified Porous Carbon.* Electroanalysis, 2020. **32**(3): p. 598-605.
76. Clifford, D.P. and J.E. Repine, *Hydrogen peroxide mediated killing of bacteria.* Molecular and cellular biochemistry, 1982. **49**(3): p. 143-149.
77. Sies, H., *Hydrogen peroxide as a central redox signaling molecule in physiological oxidative stress: Oxidative eustress.* Redox biology, 2017. **11**: p. 613-619.
78. Collin, F., *Chemical basis of reactive oxygen species reactivity and involvement in neurodegenerative diseases.* International journal of molecular sciences, 2019. **20**(10): p. 2407.
79. Song, M.-J., S.W. Hwang, and D. Whang, *Non-enzymatic electrochemical CuO nanoflowers sensor for hydrogen peroxide detection.* Talanta, 2010. **80**(5): p. 1648-1652.
80. Boubezari, I., et al., *Sensitive electrochemical detection of bioactive molecules (hydrogen peroxide, glucose, dopamine) with perovskites-based sensors.* Chemosensors, 2021. **9**(10): p. 289.
81. Mattoussi, M., F. Matoussi, and N. Raouafi, *Non-enzymatic amperometric sensor for hydrogen peroxide detection based on a ferrocene-containing cross-linked redox-active polymer.* Sensors and Actuators B: Chemical, 2018. **274**: p. 412-418.
82. Chen, W., et al., *Recent advances in electrochemical sensing for hydrogen peroxide: a review.* Analyst, 2012. **137**(1): p. 49-58.

83. Wang, Y., et al., *Direct electrochemistry and bioelectrocatalysis of horseradish peroxidase based on gold nano-seeds dotted TiO2 nanocomposite.* Biosensors and Bioelectronics, 2010. **25**(11): p. 2442-2446.
84. Xiang, C., et al., *Direct electrochemistry and enhanced electrocatalysis of horseradish peroxidase based on flowerlike ZnO–gold nanoparticle–Nafion nanocomposite.* Sensors and Actuators B: Chemical, 2009. **136**(1): p. 158-162.
85. Su, Y., et al., *Immobilization of horseradish peroxidase on amino-functionalized carbon dots for the sensitive detection of hydrogen peroxide.* Microchimica Acta, 2018. **185**: p. 1-8.
86. Wang, Y., et al., *Simple approach to fabricate a highly sensitive H2O2 biosensor by one-step of graphene oxide and horseradish peroxidase co-immobilized glassy carbon electrode.* International Journal of Electrochemical Science, 2018. **13**(3): p. 2921-2933.
87. Zhang, M., et al., *Direct electrochemistry of cytochrome c immobilized on one dimensional Au nanoparticles functionalized magnetic N-doped carbon nanotubes and its application for the detection of H2O2.* Sensors and Actuators B: Chemical, 2019. **282**: p. 85-95.
88. Norouz-Sarvestani, F., S.M. Khoshfetrat, and A. Abbaspour, *Electroreduction of Hydrogen peroxide using Direct electrocatalysis of Cytochrome c on the a graphene-modified electrode.* Nanochemistry Research, 2022. **7**(2): p. 79-84.
89. Aghamiri, Z.S., M. Mohsennia, and H.-A. Rafiee-Pour, *Immobilization of cytochrome c on polyaniline/polypyrrole/carboxylated multi-walled carbon nanotube/glassy carbon electrode: Biosensor fabrication.* Journal of Solid State Electrochemistry, 2019. **23**: p. 2233-2242.
90. Akhtar, N., et al., *Fabrication of a highly selective nonenzymatic amperometric sensor for hydrogen peroxide based on nickel foam/cytochrome c modified electrode.* Sensors and Actuators B: Chemical, 2015. **207**: p. 158-166.
91. Ren, L., et al., *Hydrogen peroxide biosensor based on direct electrochemistry of hemoglobin immobilized on gold nanoparticles in a hierarchically porous zeolite.* Microchimica Acta, 2013. **180**: p. 1333-1340.
92. Xu, X., et al., *General Preparation of Heme Protein Functional Fe3O4@ Au-Nps Magnetic Nanocomposite for Sensitive Detection of Hydrogen Peroxide.* Electroanalysis, 2017. **29**(3): p. 765-772.
93. Baghayeri, M., E.N. Zare, and M.M. Lakouraj, *Monitoring of hydrogen peroxide using a glassy carbon electrode modified with hemoglobin and a polypyrrole-based nanocomposite.* Microchimica Acta, 2015. **182**: p. 771-779.
94. Baghayeri, M. and H. Veisi, *Fabrication of a facile electrochemical biosensor for hydrogen peroxide using efficient catalysis of hemoglobin on the porous Pd@ Fe3O4-MWCNT nanocomposite.* Biosensors and Bioelectronics, 2015. **74**: p. 190-198.
95. Canbay, E., et al., *MWCNT–cysteamine–Nafion modified gold electrode based on myoglobin for determination of hydrogen peroxide and nitrite.* Bioelectrochemistry, 2015. **101**: p. 126-131.
96. Vilian, A.E., et al., *Immobilization of myoglobin on Au nanoparticle-decorated carbon nanotube/polytyramine composite as a mediator-free H2O2 and nitrite biosensor.* Scientific reports, 2015. **5**(1): p. 18390.
97. Jahanbakhshi, M., *Myoglobin immobilized on mesoporous carbon foam in a hydrogel (selep) dispersant for voltammetric sensing of hydrogen peroxide.* Microchimica Acta, 2018. **185**: p. 1-8.
98. Yoon, J., et al., *Electrochemical H2O2 biosensor composed of myoglobin on MoS2 nanoparticle-graphene oxide hybrid structure.* Biosensors and Bioelectronics, 2017. **93**: p. 14-20.
99. Xue, T., et al., *Graphene-Supported Hemin as a Highly Active Biomimetic Oxidation Catalyst.* Angewandte Chemie-International Edition, 2012. **51**(16): p. 3822-3825.
100. Le, H.T.N. and H.K. Jeong, *Electrochemical supramolecular recognition of hemin-carbon composites.* Chemical Physics Letters, 2018. **698**: p. 102-109.

101. Cao, Y., et al., *One-pot fabrication of Hemin-NC composite with enhanced electrocatalysis and application to H2O2 sensing.* Electrochimica Acta, 2018. **261**: p. 206-213.
102. Kong, F.-Y., et al., *Direct electrolytic exfoliation of graphite with hemin and single-walled carbon nanotube: Creating functional hybrid nanomaterial for hydrogen peroxide detection.* Analytica chimica acta, 2015. **884**: p. 37-43.
103. Panagiotopoulos, A., et al., *Hemin Modified SnO2 Films on ITO-PET with Enhanced Activity for Electrochemical Sensing.* Electroanalysis, 2018. **30**(9): p. 1956-1964.
104. Samourgkanidis, G., et al., *Hemin-modified SnO2/metglas electrodes for the simultaneous electrochemical and magnetoelastic sensing of H2O2.* Coatings, 2018. **8**(8): p. 284.
105. Wang, L., et al., *Cu-hemin metal-organic-frameworks/chitosan-reduced graphene oxide nanocomposites with peroxidase-like bioactivity for electrochemical sensing.* Electrochimica Acta, 2016. **213**: p. 691-697.
106. Shu, Y., et al., *Nickel metal-organic framework nanosheet/hemin composite as biomimetic peroxidase for electrocatalytic reduction of H2O2.* Journal of Electroanalytical Chemistry, 2019. **845**: p. 137-143.
107. Cheng, D., et al., *Enzyme-free Electrochemical Detection of Hydrogen Peroxide Based on the Three-Dimensional Flower-like Cu-based Metal Organic Frameworks and MXene Nanosheets.* Chinese Journal of Chemistry, 2021. **39**(8): p. 2181-2187.
108. Ghaedamini, H. and D.-S. Kim, *A non-enzymatic hydrogen peroxide biosensor based on cerium metal-organic frameworks, hemin, and graphene oxide composite.* Bioelectrochemistry, 2025. **161**: p. 108823.
109. Wu, S., et al., *Hydrothermal fabricated Ag nanoparticles-decorated reduced graphene oxide composite for H2O2 electrochemical detection.* International Journal of Electrochemical Science, 2020. **15**(7): p. 6155-6164.
110. Goud, K.Y., et al., *Polymer scaffold layers of screen-printed electrodes for homogeneous deposition of silver nanoparticles: Application to the amperometric detection of hydrogen peroxide.* Microchimica Acta, 2019. **186**(12): p. 1-10.
111. Sun, D., et al., *One-step electrodeposition of silver nanostructures on 2D/3D metal–organic framework ZIF-67: comparison and application in electrochemical detection of hydrogen peroxide.* ACS Applied Materials & Interfaces, 2020. **12**(37): p. 41960-41968.
112. Zhao, Z., et al., *Ag functionalized molybdenum disulfide hybrid nanostructures for selective and sensitive amperometric hydrogen peroxide detection.* International Journal of Electrochemical Science, 2017. **12**(9): p. 8761-8776.
113. Hu, J., et al., *An electrochemical sensor based on chalcogenide molybdenum disulfide-gold-silver nanocomposite for detection of hydrogen peroxide released by cancer cells.* Sensors, 2020. **20**(23): p. 6817.
114. Mani, V., et al., *Electrodeposition of copper nanoparticles using pectin scaffold at graphene nanosheets for electrochemical sensing of glucose and hydrogen peroxide.* Electrochimica Acta, 2015. **176**: p. 804-810.
115. Wang, K., et al., *Non-enzymatic electrochemical detection of H2O2 by assembly of CuO nanoparticles and black phosphorus nanosheets for early diagnosis of periodontitis.* Sensors and Actuators B: Chemical, 2022. **355**: p. 131298.
116. Amala, G., et al., *An environmentally benign one pot green synthesis of reduced graphene oxide based composites for the enzyme free electrochemical detection of hydrogen peroxide.* New Journal of Chemistry, 2017. **41**(10): p. 4022-4030.
117. Li, X. and X. Du, *Molybdenum disulfide nanosheets supported Au-Pd bimetallic nanoparticles for non-enzymatic electrochemical sensing of hydrogen peroxide and glucose.* Sensors and Actuators B: Chemical, 2017. **239**: p. 536-543.

118. Sangkaew, P., et al., *Emerging electrochemical sensor based on bimetallic AuPt NPs for on-site detection of hydrogen peroxide adulteration in raw cow milk.* Electrocatalysis, 2022. **13**(6): p. 794-806.
119. Oh, D.E., et al., *A flexible and transparent PtNP/SWCNT/PET electrochemical sensor for nonenzymatic detection of hydrogen peroxide released from living cells with real-time monitoring capability.* Biosensors, 2023. **13**(7): p. 704.
120. Zhao, L., et al., *Green preparation of Ag-Au bimetallic nanoparticles supported on graphene with alginate for non-enzymatic hydrogen peroxide detection.* Nanomaterials, 2018. **8**(7): p. 507.
121. Hussain, M., et al., *Ni and Co synergy in bimetallic nanowires for the electrochemical detection of hydrogen peroxide.* Nanotechnology, 2021. **32**(20): p. 205501.
122. Liu, Y., et al., *A novel non-enzymatic electrochemical biosensor based on the nanohybrid of bimetallic PdCu nanoparticles/carbon black for highly sensitive detection of H2O2 released from living cells.* Sensors and Actuators B: Chemical, 2019. **290**: p. 249-257.
123. Sharma, S., et al., *Fabrication of a non-enzymatic electrochemical sensor based on magnesium oxide nanosheets for selective and sensitive detection of hydrogen peroxide in food samples.* Journal of Applied Electrochemistry, 2024. **54**(6): p. 1365-1377.
124. Li, B., et al., *Novel neuron-network-like Cu–MoO2/C composite derived from bimetallic organic framework for highly efficient detection of hydrogen peroxide.* Analytica Chimica Acta, 2021. **1143**: p. 73-83.
125. Mani, V., et al., *Real-time quantification of hydrogen peroxide production in living cells using NiCo2S4@ CoS2 heterostructure.* Sensors and Actuators B: Chemical, 2019. **287**: p. 124-130.
126. Li, G., et al., *Portable visual and electrochemical detection of hydrogen peroxide release from living cells based on dual-functional Pt-Ni hydrogels.* Microsystems & Nanoengineering, 2023. **9**(1): p. 152.
127. Zhang, J., et al., *Assessment of salt stress to arabidopsis based on the detection of hydrogen peroxide released by leaves using an electrochemical sensor.* International Journal of Molecular Sciences, 2022. **23**(20): p. 12502.
128. Sun, L., et al., *based analytical devices for the rapid and direct electrochemical detection of hydrogen peroxide in tomato leaves inoculated with Botrytis cinerea.* Sensors, 2020. **20**(19): p. 5512.
129. Zhou, X., L. Dong, and L. Shen, *Hydroxypyridinones as a very promising platform for targeted diagnostic and therapeutic radiopharmaceuticals.* Molecules, 2021. **26**(22): p. 6997.
130. Failla, M., et al., *THP as a sensor for the electrochemical detection of H2O2.* Bioorganic Chemistry, 2024. **152**: p. 107721.
131. Lyngsie, G., et al., *Generation of hydroxyl radicals from reactions between a dimethoxyhydroquinone and iron oxide nanoparticles.* Scientific reports, 2018. **8**(1): p. 10834.
132. Lipinski, B., *Hydroxyl radical and its scavengers in health and disease.* Oxidative medicine and cellular longevity, 2011. **2011**.
133. Das, K. and A. Roychoudhury, *Reactive oxygen species (ROS) and response of antioxidants as ROS-scavengers during environmental stress in plants.* Frontiers in environmental science, 2014. **2**: p. 53.
134. Ramachandran, A. and H. Jaeschke, *Oxidative stress and acute hepatic injury.* Current Opinion in Toxicology, 2018. **7**: p. 17-21.
135. Ghaedamini, H., et al., *Reduced Glutathione-Modified Electrode for the Detection of Hydroxyl Free Radicals.* Biosensors, 2023. **13**(2): p. 254.
136. Duanghathaipornsuk, S., et al., *Detection technologies for reactive oxygen species: fluorescence and electrochemical methods and their applications.* Biosensors, 2021. **11**(2): p. 30.

137. Wu, L., et al., *Sensitive electrochemical detection of hydroxyl radical with biobarcode amplification.* Analytica chimica acta, 2012. **756**: p. 1-6.
138. Gualandi, I., et al., *A polypyrrole based sensor for the electrochemical detection of OH radicals.* Electroanalysis, 2014. **26**(7): p. 1544-1550.
139. Jabeen, E., et al., *A selective and sensitive monitoring of the OH radical using flavonoid-modified electrodes.* Electrochimica Acta, 2017. **258**: p. 228-235.
140. Fu, L., et al., *A solid-state electrochemical sensing platform based on a supramolecular hydrogel.* Sensors and Actuators B: Chemical, 2018. **262**: p. 326-333.
141. Ouyang, J., et al., *A rapid and sensitive method for hydroxyl radical detection on a microfluidic chip using an N-doped porous carbon nanofiber modified pencil graphite electrode.* Analyst, 2014. **139**(13): p. 3416-3422.
142. Cadet, J. and J.R. Wagner, *Oxidatively generated base damage to cellular DNA by hydroxyl radical and one-electron oxidants: similarities and differences.* Archives of biochemistry and biophysics, 2014. **557**: p. 47-54.
143. Huang, Y., et al., *Real time detection of hazardous hydroxyl radical using an electrochemical approach.* ChemistrySelect, 2019. **4**(43): p. 12507-12511.
144. Wu, L., et al., *Sensitive electrochemical detection of hydroxyl radical with biobarcode amplification.* Anal Chim Acta, 2012. **756**: p. 1-6.
145. Abdel-Hamid, R. and E.F. Newair, *Electrochemical behavior of antioxidants: Part 3. Electrochemical studies of caffeic Acid–DNA interaction and DNA/carbon nanotube biosensor for DNA damage and protection.* Arabian Journal of Chemistry, 2016. **9**(3): p. 365-370.
146. Hájková, A., J. Barek, and V. Vyskočil, *Electrochemical DNA biosensor for detection of DNA damage induced by hydroxyl radicals.* Bioelectrochemistry, 2017. **116**: p. 1-9.
147. Musialik, M., et al., *Acidity of hydroxyl groups: an overlooked influence on antiradical properties of flavonoids.* The Journal of organic chemistry, 2009. **74**(7): p. 2699-2709.
148. Sestili, P., et al., *Quercetin prevents DNA single strand breakage and cytotoxicity caused by tert-butylhydroperoxide: free radical scavenging versus iron chelating mechanism.* Free Radical Biology and Medicine, 1998. **25**(2): p. 196-200.
149. Xu, Y., et al., *A novel electrochemical sensor for determination of hydroxyl radicals in living cells by coupling nanoporous gold layer with self-assembled 6-(Ferrocenyl) hexanethiol.* Analytica Chimica Acta, 2020. **1096**: p. 69-75.
150. Xu, Y., et al., *A novel electrochemical sensor for determination of hydroxyl radicals in living cells by coupling nanoporous gold layer with self-assembled 6-(Ferrocenyl) hexanethiol.* Anal Chim Acta, 2020. **1096**: p. 69-75.
151. Ding, S., et al., *Sensitive and selective measurement of hydroxyl radicals at subcellular level with tungsten nanoelectrodes.* Analytical chemistry, 2020. **92**(3): p. 2543-2549.
152. Giustarini, D., et al., *Oxidative stress and human diseases: origin, link, measurement, mechanisms, and biomarkers.* Critical reviews in clinical laboratory sciences, 2009. **46**(5-6): p. 241-281.
153. Qin, J., et al., *Preparation of molecularly imprinted electrochemical sensors for selective detection of hydroxyl radicals based on reduced graphene oxide nanosilver (rGO/AgNPs) composites.* Microchemical Journal, 2024: p. 110006.
154. Huang, Z., et al., *Molecularly imprinted polymer functionalized reduced graphene oxide: a new platform for the detection of hydroxyl radicals in the atmosphere.* Analytical Methods, 2019. **11**(40): p. 5126-5133.
155. Huang, Z., et al., *Salicylic acid impregnated activated carbon fiber paper: An effective platform for the simple and sensitive detection of hydroxyl radicals in the atmosphere.* Electrochemistry Communications, 2019. **100**: p. 113-116.

156. Huang, Z., Q. Xu, and X. Hu, *Covalent organic frameworks functionalized carbon fiber paper for the capture and detection of hydroxyl radical in the atmosphere.* Chinese Chemical Letters, 2020. **31**(9): p. 2495-2498.
157. Duanghathaipornsuk, S., et al., *Detection of Hydroxyl Radicals Using Cerium Oxide/Graphene Oxide Composite on Prussian Blue.* Nanomaterials, 2020. **10**(6): p. 1136.
158. Duanghathaipornsuk, S., et al., *Detection of Hydroxyl Radicals Using Cerium Oxide/Graphene Oxide Composite on Prussian Blue.* Nanomaterials (Basel), 2020. **10**(6): p. 1136.
159. Duanghathaipornsuk, S., et al., *The effects of size and content of cerium oxide nanoparticles on a composite sensor for hydroxyl radicals detection.* Sensors and Actuators B: Chemical, 2020. **321**: p. 128467.
160. Duanghathaipornsuk, S., et al., *Supersensitive CeO x-based nanocomposite sensor for the electrochemical detection of hydroxyl free radicals.* Nanoscale, 2021. **13**(9): p. 5136-5144.
161. Hassan, M.H., D. Andreescu, and S. Andreescu, *Cerium Oxide Nanoparticles Stabilized within Metal–Organic Frameworks for the Degradation of Nerve Agents.* ACS Applied Nano Materials, 2020. **3**(4): p. 3288-3294.
162. Ghaedamini, H., A.C. Alba-Rubio, and D.-S. Kim, *A Novel Electrochemical Sensor Based on a Cerium Oxide/Gold/Carbon Nanocompositefor the Detection of Hydroxyl Free Radicals.* Journal of The Electrochemical Society, 2023.
163. Sinha, A., et al., *Polymer hydrogel interfaces in electrochemical sensing strategies: A review.* TrAC Trends in Analytical Chemistry, 2019. **118**: p. 488-501.
164. Matai, I. and P. Gopinath, *Chemically cross-linked hybrid nanogels of alginate and PAMAM dendrimers as efficient anticancer drug delivery vehicles.* ACS Biomaterials Science & Engineering, 2016. **2**(2): p. 213-223.
165. Hu, Y., J.-O. You, and J. Aizenberg, *Micropatterned hydrogel surface with high-aspect-ratio features for cell guidance and tissue growth.* ACS applied materials & interfaces, 2016. **8**(34): p. 21939-21945.
166. Wang, Z., L. Zhang, and Y. Tian, *A durable non-enzymatic electrochemical sensor for monitoring H 2 O 2 in rat brain microdialysates based on one-step fabrication of hydrogels.* Analyst, 2015. **140**(11): p. 3788-3793.
167. Kumar, V., A. Sachdev, and I. Matai, *Self-assembled reduced graphene oxide–cerium oxide nanocomposite@ cytochrome c hydrogel as a solid electrochemical reactive oxygen species detection platform.* New Journal of Chemistry, 2020. **44**(26): p. 11248-11255.

No primary research results, software or code have been included and no new data were generated or analyzed as part of this review.